doi:10.1093/brain/awt336 Brain 2014: 137; 739–756 | 739

BRAIN
A JOURNAL OF NEUROLOGY

# Rewiring of the corticospinal tract in the adult rat after unilateral stroke and anti-Nogo-A therapy

**Nicolas T. Lindau, Balthasar J. Bänninger, Miriam Gullo, Nicolas A. Good, Lukas C. Bachmann, Michelle L. Starkey* and Martin E. Schwab**

Brain Research Institute, University of Zurich and Department of Health Science and Technology Swiss Federal Institute of Technology Zurich, Switzerland

*Present address: Paraplegic Centre, Balgrist University Hospital Zurich, Switzerland

Correspondence to: Nicolas Thomas Lindau
Brain Research Institute,
University and ETH Zurich,
Winterthurerstrasse 190
8057 Zurich,
Switzerland
E-mail: lindau@hifo.uzh.ch

**Adult Long Evans rats received a photothrombotic stroke that destroyed >90% of the sensorimotor cortex unilaterally; they were subsequently treated intrathecally for 2 weeks with a function blocking antibody against the neurite growth inhibitory central nervous system protein Nogo-A. Fine motor control of skilled forelimb grasping improved to 65% of intact baseline performance in the anti-Nogo-A treated rats, whereas control antibody treated animals recovered to only 20% of baseline scores. Bilateral retrograde tract tracing with two different tracers from the intact and the denervated side of the cervical spinal cord, at different time points post-lesion, indicated that the intact corticospinal tract had extensively sprouted across the midline into the denervated spinal hemicord. The original axonal arbours of corticospinal tract fibres that had recrossed the midline were subsequently withdrawn, leading to a complete side-switch in the projection of a subpopulation of contralesional corticospinal tract axons. Anterograde tracing from the contralesional cortex showed a 2–3-fold increase of midline crossing fibres and additionally a massive sprouting of the pre-existing ipsilateral ventral corticospinal tract fibres throughout the entire cervical enlargement of the anti-Nogo-A antibody-treated rats compared to the control group. The laminar distribution pattern of the ipsilaterally projecting corticospinal tract fibres was similar to that in the intact spinal cord. These plastic changes were paralleled by a somatotopic reorganization of the contralesional motor cortex where the formation of an ipsilaterally projecting forelimb area was observed. Intracortical microstimulation of the contralesional motor cortex revealed that low threshold currents evoked ipsilateral movements and electromyography responses at frequent cortical sites in the anti-Nogo-A, but not in the control antibody-treated animals. Subsequent transection of the spared corticospinal tract in chronically recovered animals, treated with anti-Nogo-A, led to a reappearance of the initial lesion deficit observed after the stroke lesion. These results demonstrate a somatotopic side switch anatomically and functionally in the projection of adult corticospinal neurons, induced by the destruction of one sensorimotor cortex and the neutralization of the CNS growth inhibitory protein Nogo-A.**

**Keywords:** stroke; anti-Nogo-A; somatotopic reorganization; plasticity; midline crossing fibres
**Abbreviations:** BrdU = bromodeoxyuridine; CST = corticospinal tract

Received July 16, 2013. Revised October 16, 2013. Accepted October 18, 2013. Advance Access publication December 18, 2013
© The Author (2013). Published by Oxford University Press on behalf of the Guarantors of Brain. All rights reserved.
For Permissions, please email: journals.permissions@oup.com

# Introduction

Stroke is the leading cause of persistent neurological disability in the elderly population worldwide (Bakhai, 2004; Donnan *et al.*, 2008). Small stroke lesions, where <10–15% of the cortex is destroyed unilaterally, often show good spontaneous recovery within days and weeks (Liepert *et al.*, 2000; Cramer, 2008; Starkey *et al.*, 2012), accompanied with a plastic reorganization of nearby areas, larger stroke lesions, where >60% of the cortex is destroyed unilaterally, often result in permanent neurological deficits (Biernaskie *et al.*, 2005). Such larger lesions have been shown to be accompanied by a somatotopic reorganization of more remote areas, such as the contralesional motor- and premotor cortex in humans and in experimental animals (Johansen-Berg *et al.*, 2002; Biernaskie *et al.*, 2005; Bestmann *et al.*, 2010; Rehme *et al.*, 2011). However, if such a lesion happens early in life, in the plastic developmental CNS, as observed in children with a congenital hemiparesis or hemispherectomy, reorganization of the contralesional hemisphere is often correlated with good recovery of function (Choi *et al.*, 2009; Lotze *et al.*, 2009). For these patients a functional shift, so that the unlesioned hemisphere controlled both sides of the body, was observed. Similar observations were made in neonatally operated animals, accompanied by an anatomical reorganization of the descending, spared corticospinal tract (CST) which involved fibres recrossing the midline, as well as the sprouting of pre-existing ipsilateral CST fibres (Kartje-Tillotson *et al.*, 1987; Rouiller *et al.*, 1991; Fujimura *et al.*, 2003; Umeda and Isa, 2011). In adult stroke patients, abnormal activation of contralesional cortical areas was sometimes correlated with poor outcomes (Murase *et al.*, 2004; Nowak *et al.*, 2009), but due to recent high resolution imaging and stimulation techniques, more and more studies describe a correlation between functional recovery and somatotopic reorganization of the unlesioned hemisphere (Chollet *et al.*, 1991; Johansen-Berg *et al.*, 2002; Schaechter and Perdue, 2008; Bestmann *et al.*, 2010; Stoeckel and Binkofski, 2010; Rehme *et al.*, 2011; Grefkes and Ward, 2013). However, this is still a matter of debate and the size and precise location of the lesion play crucial roles that require more detailed investigation.

Exercise-driven rehabilitation training, like constraint-induced movement therapy, has been shown to enhance plastic rearrangements and increase functional recovery even in adult stroke patients and animals (Taub and Uswatt, 2006; Maier *et al.*, 2008). Furthermore, in experimental animal models several growth-promoting treatments have been shown to increase the number of midline crossing CST fibres in the spinal cord and to enhance behavioural recovery after stroke. These treatments include function blocking antibodies against the neurite growth inhibitory CNS protein Nogo-A (Emerick *et al.*, 2003; Seymour *et al.*, 2005; Hamadjida *et al.*, 2012), *Nogo* (now known as *RTN4*) knockout mice (Kim *et al.*, 2003; Simonen *et al.*, 2003), reagents blocking the Nogo receptor NgR1 (now known as RTN4R) (Lee *et al.*, 2004; Kubo *et al.*, 2008), digestion of chondroitin sulphate proteoglycans with chondroitinase ABC (Soleman *et al.*, 2012; Harris *et al.*, 2013), and high doses of the sugar inosine (Chen *et al.*, 2002). An important aspect of the anti-Nogo/Nogo-receptor treatments concerns their temporal window of opportunity. In contrast with the narrow time window of a few hours for the conventional recombinant tissue plasminogen activator (rt-PA) treatment, anti-Nogo-A antibodies were shown to be fully efficacious even when applied 9 weeks after the stroke in adult rats (Wiessner *et al.*, 2003; Tsai *et al.*, 2010; Kumar and Moon, 2013). However, many open questions regarding a correlation between improved recovery and plastic reorganization, especially the location of ipsilaterally projecting cells in the cortex, possible bilaterally projecting cells and the functionality of new projections after stroke remain. In this study, we used the highly controllable photothrombotic stroke model in adult rats, in combination with anterograde and retrograde tracing techniques, electrophysiology and behavioural analyses to investigate spontaneous and anti-Nogo-A antibody-induced functional recovery and to correlate this with the anatomical reorganization of the contralesional hemisphere and its descending CST over the course of 1 to 12 weeks after the injury.

# Materials and methods

## Animals

Adult, female Long Evans rats ($n = 129$; 230–400 g, 3–7 months of age, Charles River) were used in this study. Female animals were used as they are less aggressive and learn the single pellet grasping task more easily. Animals were housed in groups of three to four under a constant 12 h light/dark cycle with food and water *ad libitum*. All experimental procedures (Supplementary Figs 1–3) were approved by the veterinary office of the canton of Zurich, Switzerland.

## Anaesthesia and postoperative care

For all surgical procedures, except intracortical microstimulation, animals were anaesthetized with 3% isoflurane followed by a subcutaneous injection of a mixture of Hypnorm® (600 µl/kg body weight, Janssen Pharmaceutics) and Dormicum® (3.75 mg/kg body weight, Roche Pharmaceuticals). For intracortical microstimulation a mixture of ketamine (50 mg/ml, 7 mg/kg body weight, Streuli Pharma) and xylazine (20 mg/ml, 5 mg/kg body weight, Streuli Pharma) was injected intramuscularly with additional top-up of ketamine when needed. After the surgery all animals received postoperative care including analgesics (Rimadyl®, 2.5 mg/kg body weight, Pfizer) and antibiotics (Baytril®, 5 mg/kg body weight, Bayer) for 3 days. After a stroke lesion animals additionally received a single subcutaneous injection of mannitol (20%, 17 ml/kg, B. Braun) to reduce swelling of the cortex. After surgery, animals were warmed on a heating pad for 24 h before being transferred back to the animal facility.

## Photothrombotic stroke and antibody application

A photothrombotic stroke was induced in 116 animals ($n = 59$ control antibody treatment, $n = 57$ anti-Nogo-A antibody treatment) to unilaterally lesion the sensorimotor cortex as previously described (Watson *et al.*, 1985; Wiessner *et al.*, 2003). Briefly the animal was fixed in a stereotactic frame and the skull was exposed and cleaned.

An opaque template with an opening for the light source (10 × 5 mm) was positioned on the side of the cortex contralateral to the preferred paw (see 'Behaviour' section). The opening of the template was positioned 5 mm to −5 mm anterior and 0.5 mm to 5.5 mm lateral relative to bregma. A fibreglass light with 10 mm diameter was placed directly over the exposed skull. A mixture of Rose Bengal in saline (13 mg/kg body weight, 10 mg/ml Rose Bengal in 0.9% NaCl solution) was injected through a catheter in the femoral vein, and after 2 min the skull was illuminated (Olympus KL1500LCD, 150 W, 3000 K) for 10 min at the maximum output of the light source. The catheter was then carefully removed and the animal was detached from the frame and sutured.

For the antibody application (Weinmann *et al.*, 2006) a laminectomy was performed at the lumbar level L2 during the same anaesthesia as for the stroke. A fine intrathecal catheter (32 gauge) was placed in the subarachnoid space and connected to an osmotic minipump (Alzet® 2ML2; 5 µl/h, 3.1 µg/µl) for constant delivery of the function blocking IgG1 mouse monoclonal anti-Nogo-A antibody 11C7 (3 mg/ml, Novartis) (Oertle *et al.*, 2003; Liebscher *et al.*, 2005) or the monoclonal control antibody, anti-bromodeoxyuridine (BrdU; 3 mg/ml, AbD Serotec). After 2 weeks the pump and catheter were removed and the animal was sutured. Animals were number-coded and investigators were always blinded to the treatment groups until the end of the data analysis.

## Behaviour

Nineteen animals ($n = 10$ control antibody treatment, $n = 9$ anti-Nogo-A antibody treatment) were used in the single pellet grasping test to assess the recovery of fine motor skills of the forelimb after photothrombotic stroke and treatment (Whishaw and Pellis, 1990). Animals were food deprived the day before testing to increase their motivation. The rat was placed in a Plexiglas box (34 × 14 cm) with two openings on opposite sides. The animal was trained to reach for a sugar pellets (45 mg dustless precision pellet, TSE Systems Int. Group), alternately at both openings of the box, and bring them to their mouth. The first training sessions were used to identify the paw preference of the animal, and once established, testing was always performed on this side. The grasping success of the animals was scored during a maximum time of 10 min where the animals could grasp for 20 pellets. A score of 1 was given when the animal was able to reach out for the pellet and bring it to the mouth. If the animal dropped the pellet inside the box before bringing it to its mouth, a score of 0.5 was given. If the rat knocked the pellet off the shelf without retrieving it, a score of 0 was given. The success rate was calculated for each animal as the sum of the pellet scores (eaten and dropped) divided by the pre-lesion baseline score (eaten and dropped) multiplied by 100; normalizing the success rate of each animal to the baseline performance. Animals were trained daily for ∼3 weeks and only animals able to successfully grasp >10 of 20 pellets were included in the study. Post-operation, the animals were tested at Days 3 and 7, and from then on, once a week until Day 84. In addition, each testing session was filmed (Panasonic HDC-SD800 High Definition Camcorder) and evaluated using frame-by-frame video analysis at a later date (VideoReDo TV Suite, H.264, DRD Systems Inc.). Briefly, three grasps were evaluated after the 10-point evaluation skilled reaching score: digits to midline, digits semi flexed, elbow to midline, advance, digits extend, pronation, grasp, supination I and II and release (Farr and Whishaw, 2002; Metz *et al.*, 2005). A score of 0 was given for a normal movement, a score of 1 was given for an impaired movement and a score of 0.5 was given for a slightly impaired movement.

## Retrograde tracing

Retrograde tracing was performed in 70 animals, of which four animals were excluded from the study because of a spread of tracer over the midline ($n = 2$ anti-Nogo-A treated animals and $n = 2$ naive animals). With the remaining animals, multiple time points after stroke were investigated: six naive animals, 31 anti-BrdU treated animals (10 days postoperative $n = 7$, 21 days postoperative $n = 7$, 30 days postoperative $n = 5$, 42 days postoperative $n = 6$, 84 days postoperative $n = 6$) and 29 anti-Nogo-A treated animals (10 days postoperative $n = 7$, 21 days postoperative $n = 6$, 30 days postoperative $n = 5$, 42 days postoperative $n = 5$, 84 days postoperative $n = 6$). Briefly, a laminectomy was performed at the cervical spinal level C7 to C8 and the animal was fixed to a stereotactic frame by holding the dorsal processes, rostral and caudal of the laminectomy. The dura was opened carefully and folded aside. Ten injections of Diamidino Yellow (2% suspension in 0.1 M phosphate buffer with 2% dimethyl sulphoxide, Sigma) were made ipsilateral to the lesion and afterwards 10 injections of Fast Blue (2% suspension in 0.1 M phosphate buffer with 2% dimethylsulphoxide, EMS-Chemie) were made contralateral to the lesion. This injection pattern allowed us to use the slightly more efficient tracer Fast Blue to label the rare ipsilateral projecting fibres (Reinoso and Castro, 1989; Puigdellivol-Sanchez *et al.*, 2000). A 28-gauge, 10 µl syringe (Hamilton, BGB Analytik) driven by an electrical pump (World Precision Instruments) with a flow rate of 170 nl/s was used for each injection consisting of 120 nl tracer. The first injection was made most caudally at C8 and was positioned 0.8 mm from the midline in a depth of 1.2 mm. Two minutes after the injection the needle was retracted and positioned 0.5 mm rostral for the next injection. This procedure was repeated for all injections. The tracer was transported for 4 days before the animal was perfused. All injection sites were carefully checked on coronal cross-sections of the spinal cord for a possible spread of tracer over the midline. Animals were strictly excluded whenever a spread of tracer was observed.

## Anterograde tracing

Anterograde tracing was performed 70 days after stroke in 16 animals ($n = 8$ anti-BrdU and $n = 8$ anti-Nogo-A treated animals). Briefly, the animals were fixed in a stereotactic frame, the scalp was opened and a craniotomy was performed over the intact motor cortex of the contralesional side (0–5 mm anterior and 0–4 mm lateral relative to bregma) exposing the forelimb area. Two stereotactic injections of the anterograde tracer tetramethylrhodamine-dextran (10% in $H_2O$, 10 000 MW, Fluoro Ruby, Invitrogen) were made into the rostral forelimb area (3.5 mm anterior/2 mm lateral; 3.5 mm anterior/2.5 mm lateral relative to bregma) and four injections of fluorescein-biotin-dextran (10% in $H_2O$, 10 000 MW, Mini Emerald, Invitrogen) were made into the caudal forelimb area (1.5 mm anterior/2.5 mm lateral; 1.5 mm anterior/3 mm lateral; 1 mm anterior/ 2.5 mm lateral and 1 mm anterior/3 mm lateral; all coordinates relative to bregma). All injections were made at a depth of 1.5 mm relative to the surface of the cortex. The injections were made through the intact dura with a 35-gauge, 10 µl syringe (World Precision instruments) controlled by an electrical pump (World Precision Instruments). Each injection consisted of 200 nl of tracer at a flow rate of 6 nl/s. The needle remained in place for 2 min after each injection to avoid backflow of the tracer. After the last injection the animal was sutured and removed from the stereotactic frame. The tracer was transported for 2 weeks (chronic time point 84 days after lesion) before the animal was perfused.

## Intracortical microstimulation

Twenty-four animals were used for intracortical microstimulation: five naive animals, 10 anti-BrdU-treated animals (21 days postoperative $n = 4$, 84 days postoperative $n = 6$) and nine anti-Nogo-A treated animals (21 days postoperative $n = 4$, 84 days postoperative $n = 5$). Briefly, animals were anaesthetized with ketamine/xylasine (see above), the forelimbs were shaved for better visibility of muscles and the rat was mounted in a stereotactic frame (Neafsey *et al.*, 1986; Emerick *et al.*, 2003). The scalp was opened and a craniotomy was performed on the contralesional side exposing the entire motor cortex (5 mm to − 4 mm anterior and 5 mm lateral relative to bregma). Immediately afterwards a single subcutaneous injection of mannitol (20%, 17 ml/kg, B. Braun) was given to reduce swelling of the cortex. The dura was kept intact and warm Ringer solution (Fresenius) was used to keep the brain moist. Using bregma as a cranial landmark, randomized electrode penetrations were made perpendicular to the pial surface (depth 1.3–1.9 mm). The exploration grid covered the entire area of the motor cortex (100–120 stimulation points with around 40 forelimb responses per animal) with a minimum distance of 400 μm for each stimulation point. Forty-five-millisecond trains of 0.2 ms biphasic pulses at 333 Hz were delivered through a glass isolated platinum/tungsten stimulation electrode with an impedance of 1–2 MΩ (Thomas Recording). EMG recordings from the ipsilateral and contralateral forelimb (M. trapezius for shoulder, M. biceps and triceps brachii for elbow and M. extensor digitorum for wrist and finger movements) were used as readout. Stimulation was considered successful if a movement/EMG response was evoked with a current of $\leqslant 80$ μA (Emerick *et al.*, 2003; Brus-Ramer *et al.*, 2007). If a movement/EMG was detected, the current was reduced to define the lowest threshold inducing a response. Threshold was always defined from two ways; coming from a higher current down to a lower current and additionally coming from a lower current upwards. One investigator (blinded to the treatment group and the EMG response) applied the stimulation current, while the other experimenter (blinded to the treatment and the position of the electrode) assessed EMG response. For each stimulation site the lowest current threshold where a forelimb response was observed was determined. The side of the movement (ipsi- and/or contralateral), the type of movement (shoulder/elbow/wrist) and the current was analysed for each coordinate. If a bilateral EMG response was observed at high current strengths, the current thresholds for contra- and ipsilateral responses were recorded independently. The EMG signal was amplified, filtered, digitized and visualized via PowerLab (AD Instruments).

## Pyramidotomy

The 19 animals used for behavioural testing ($n = 10$ anti-BrdU, $n = 9$ anti-Nogo-A) received, additionally, a unilateral transection of the contralesional CST, which had been spared from the photothrombotic stroke, as described previously (Thallmair *et al.*, 1998; Starkey *et al.*, 2011). Briefly, the medullary pyramids were surgically exposed using a ventral approach. The trachea was exposed and together with the oesophagus carefully displaced laterally. The midline surface of the occipital bone was uncovered by blunt dissection and a small hole was drilled just lateral to the midline exposing the medullary pyramids and the basilar artery. The dura was opened and a fine tungsten needle was lowered to 1 mm below the surface of the pyramids. The needle was displaced laterally and towards the midline and gently lifted to avoid rupture of blood vessels. The opening was closed by suturing superficial muscles and the skin.

## Perfusion and tissue preparation

All animals were transcardially perfused with 100 ml Ringer solution [containing 100 000 IU/l heparin (Roche) and 0.25% $NaNO_2$] followed by 300 ml of a 4% phosphate-buffered paraformaldehyde solution containing 5% sucrose. The brain and spinal cord were dissected and post-fixed overnight in the same solution at 4°C, before being cryoprotected in a phosphate-buffered 30% sucrose solution for 7 days at 4°C. The brain and spinal cord were embedded in Tissu-Tek® O.C.T.™ and frozen in isopentane (Sigma) at −40°C. Brains were cut coronally on a cryostat in 40 μm thick sections, whereas spinal cords were cut coronally into 50 μm thick sections. Sections were collected on slides (SuperFrost®) before being coverslipped with Mowiol® mounting medium (Calbiochem).

## PKC-$\gamma$ staining

For animals which received a pyramidotomy ($n = 10$ anti-BrdU, $n = 9$ anti-Nogo-A) an immunostaining with an antibody raised against PKC-$\gamma$ was used to assess the completeness of the pyramidotomy lesion, as described previously (Mori *et al.*, 1990). Briefly, 50 μm sections were incubated with a rabbit anti-PKC-$\gamma$ at 1:200 (Santa Cruz Biotechnology) overnight. After rinsing, the primary antibody was detected with a secondary goat anti-rabbit Cy3 coupled antibody at 1:300 (Molecular Probes, Invitrogen) for 2 h. Sections were coverslipped in Mowiol® mounting medium (Calbiochem) and visualized under a Zeiss fluorescent microscope. For quantification of the lesion, the staining intensity of the superficial dorsal horn (unaffected by lesion) was compared with the staining intensity of the dorsal CST.

## Quantification of anterograde tracing

Mosaic pictures of every ninth spinal cord cross section were obtained through the entire cervical spinal cord (C2–T1) (Zeiss Axioskop 2MOT with motorized stage, ×200) for further analysis. For both anterograde tracers, fluorescein and tetramethylrhodamine, the amount of midline crossing fibres and white/grey matter crossings of pre-existing ipsilateral/ventral CST fibres were counted (ImageJ) and normalized against the number of fibres in the intact dorsal CST at the cervical level C2. For midline crossing fibres a virtual line was placed at a tangent to the border of the central canal contralateral to the traced dorsal CST. It was aligned with the anterior median fissure of the spinal cord and the boundary of traced and untraced dorsal CST. Fibres were counted as midline crossing fibres when they crossed this virtual line. Ventral CST fibres were counted at the transition of the white matter forming the anterior median fissure and the grey matter of the ventral horn. A virtual line was aligned with the centre of the central canal. Around this point the line was rotated and aligned with the boundary between grey and white matter. Fibres crossing this line were counted as ventral CST fibres innervating the grey matter. To investigate the spatial distribution of contra- and ipsilateral projecting CST fibres throughout the spinal cord laminae, the position of each fibre within the spinal cord grey matter at the cervical level C4 was manually drawn using Photoshop (CS4) (two sections per animal). Each section, including the fibre drawings, was adapted to a standard spinal cord template (Paxinos and Watson, 2005) of the cervical level C4. The fibre density and distribution was analysed as grey-scale densitometry of fibre drawings, and Matlab (R2011b) was used to create false colour coded heat-maps for anti-Nogo-A and control antibody treated animals. This intermediate step of manual fibre drawing was necessary, as the fluorescent tracers induced too much unspecific background for an automated image analysis.

## Quantification of retrograde tracing

The number of Fast Blue, Diamidino Yellow and double-labelled cells was counted on every third section for the entire cortex of each animal (magnification $\times 100$). For the chronic time points (84 days post-lesion), 3D reconstructions of the brain surface, the lesion size and the location of the labelled neurons were obtained from every ninth section using Neurolucida 8.0 (MicroBrightField) and Matlab (R2011b).

## Statistics

For comparing the behavioural recovery of the two treatment groups, a two-way ANOVA followed by Bonferroni's *post hoc* test was used (Figs 1 and 7). The same test was also applied when the distribution of cells (retrograde tracing) or fibres (anterograde tracing) was investigated over a distance/time (Figs 3 and 5). Whenever the two treatments were compared at one time point (bar-plot), Student's *t*-test (two-tailed, unpaired) was used (Figs 2, 5 and 6). For parts of the intracortical microstimulation analysis it was necessary to use a one sample *t*-test against a theoretical mean, as the anti-BrdU group did not have one positive ipsilateral EMG response (Fig. 6). Data are presented as mean ± standard error of the mean (SEM) with asterisks indicating significance: $*P \leqslant 0.05$; $**P \leqslant 0.01$ and $***P \leqslant 0.001$.

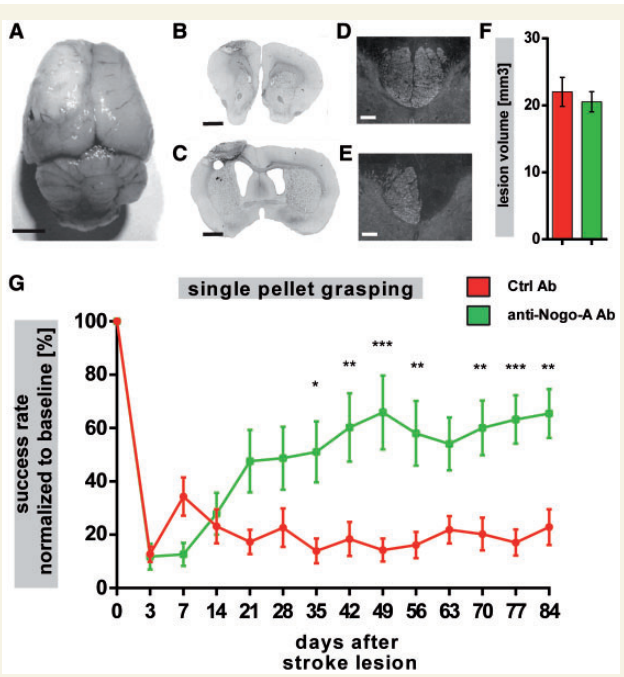


**Figure 1** Functional recovery in the single pellet grasping task after unilateral photothrombotic stroke lesion. Dorsal view (**A**) and coronal section (**B** and **C**) of a brain with photothrombotic stroke. (**D** and **E**) Representative cross sections of the cervical spinal cord stained for the CST marker PKC-$\gamma$ of a naive animal (**D**) and an animal with stroke (84 days post-stroke) (**E**). The lesion volume of the two treatment groups (**F**) was evaluated by 3D reconstruction of every ninth brain section, using Neurolucida 8.0 (MicroBrightField). Lesion volume was used as readout for all animals that did not receive bilateral retrograde tracing (control antibody, $n = 28$ and anti-Nogo-A, $n = 26$) for assessing lesion position and size. Success rate in the single pellet grasping task at baseline (intact, trained) and after an unilateral photothrombotic stroke to the sensorimotor cortex of the preferred paw (**G**) and treatment with a control antibody (red, $n = 10$) or an anti-Nogo-A antibody (green, $n = 9$). Data are presented as means ± SEM. Statistical evaluation was carried out with two-way ANOVA repeated measure followed by Bonferroni *post hoc*, asterisks indicate significances: $*P < 0.05$, $**P < 0.01$ and $***P < 0.001$. Scale bars: **A** = 5 mm; **B** and **C** = 2 mm; **D** and **E** = 50 μm.

# Results

## Lesion position and size

Lesion size and position was evaluated by 3D reconstruction of the brain, using Neurolucida 8.0 (MicroBrightField) for all animals that did not receive bilateral retrograde tracing (control antibody, $n = 28$ and anti-Nogo-A, $n = 26$) (Fig. 1F and Supplementary Fig. 1). Additionally, for all retrograde traced animals the number and position of surviving CST neurons with intact connections to the contralateral cervical spinal cord (Fast Blue-positive cells) in the ipsilesional cortex was determined (Figs 2I and 3A). The lesion affected almost all layers of the entire motor cortex unilaterally, the corpus callosum, partially subcortical structures like the striatum (Fig. 1A–C) and led to a complete degeneration of the affected CST (Fig. 1D and E). Only ~4–9% of Fast Blue-labelled cells were left in the ipsilesional motor cortex (Fig. 2I), mainly located in the most lateral rim region and the most rostral part of the rostral forelimb area (Figs 2E and 3A, and Supplementary Fig. 1). No difference in lesion size (anti-BrdU = 22.03 ± 2.17 $mm^3$, anti-Nogo-A = 20.54 ± 1.5 $mm^3$) or amount of remaining Fast Blue-labelled cells and their location was observed for the two groups (anti-BrdU = 404 ± 49 Fast Blue cells, anti-Nogo-A = 551 ± 77 Fast Blue cells; $P > 0.05$, unpaired two-tailed Student's *t*-test).

## Functional recovery of skilled forelimb grasping after stroke and treatment with an anti-Nogo-A antibody

Animals were tested in the single pellet grasping task to assess recovery of fine motor skills (Whishaw and Pellis, 1990) after stroke and treatment with an anti-Nogo-A antibody (11C7) or control antibody (anti-BrdU). At Day 3 post-lesion all animals showed a massive and comparable drop in the success rate of pellet grasping (13% ± 3% for anti-BrdU, 12% ± 5% for anti-Nogo-A). From Day 7 onward, the performance of the anti-Nogo-A antibody treated animals constantly improved, reaching a final, stable success rate of 65% ± 9% at Days 49–84 after lesion (Fig. 1G). The success rate of the anti-BrdU treated animals plateaued around Day 14 at a low level of performance and showed no further improvement until Day 84 (24% ± 6%). The recovery was significantly different for both groups, with the anti-Nogo-A animals out-performing the control antibody treated animals at every time point from 21 days post-lesion onwards ($P < 0.01$, two-way repeated measures ANOVA). The 10-point evaluation skilled reaching score showed a more normal grasping

performance of anti-Nogo-A treated animals compared with control antibody treated animals (Supplementary Fig. 2). Control antibody-treated animals showed impairment in almost every aspect of the grasping movement, whereas anti-Nogo-A treated animals only had impairments in the supination of the grasping movement.

## Somatotopic reorganization of the contralesional hemisphere caused by a 'side switch' of the descending corticospinal projections after stroke

Two different retrogradely transported dyes were injected into the denervated (Fast Blue) and intact (Diamidino Yellow) side of the spinal cord in intact (naive) animals, and at 10, 21, 30, 42 and 84 days after the stroke. Numbers of single- and double-labelled cells on the contralesional and ipsilesional side of the sensorimotor cortex were determined (Fig. 2A–E). For naive animals, $9198 \pm 410$ Fast Blue-labelled cells were detected on the side contralateral to the injection. This number declined massively after the stroke lesion when only ~4–9% of Fast Blue-labelled cells were left in the ipsilesional motor cortex, mainly located in the most lateral rim region and the most rostral part of the rostral forelimb area (Fig. 2E and I). No change over time was detected for either of the two treatment groups (anti-BrdU and anti-Nogo-A) ($P > 0.05$, unpaired two-tailed Student's *t*-test).

For the second tracer, $4621 \pm 752.3$ Diamidino Yellow retrogradely-labelled cortical cells were detected in naive animals on the side contralateral to the injection, making Diamidino Yellow roughly half as sensitive as Fast Blue. After a photothrombotic stroke, both treatment groups showed no significant changes of Diamidino Yellow-labelled cells in the contralesional cortex until Day 42 post-lesion. For the chronic time point (Day 84) a significant increase was observed for both lesion groups ($8099 \pm 563.7$ anti-BrdU, $7821 \pm 764$ anti-Nogo-A), but no significant difference existed between the groups (Fig. 2J).

To study the existence of bilaterally projecting neurons, we evaluated double-labelled cells that had taken up both retrograde tracers, Fast Blue and Diamidino Yellow (Fig. 2B and F–H). In naive animals only $18 \pm 2$ double-labelled cells were observed on the side of the contralaterally projecting Diamidino Yellow-labelled cells (Fig. 2K). After stroke the control antibody-treated group showed a decrease of double-labelled cells which returned to naive levels at the chronic time point ($12 \pm 2$ double-labelled cells). For the anti-Nogo-A antibody-treated animals a marked increase of double-labelled cells was observed which peaked at Day 21 post-lesion (Fig. 2K), indicating a massive sprouting of intact CST fibres over the spinal cord midline. The increase of double-labelled cells was 2.4-fold and significantly different from anti-BrdU treated animals ($P < 0.001$, unpaired two-tailed Student's *t*-test). Interestingly, the time point of the peak (21 days post-lesion) correlated with the time point where the anti-Nogo-A treated animals started to outperform the anti-BrdU treated animals in the single pellet grasping task (Fig. 1G). After the initial peak of double-labelled cells at Day 21 post-lesion a rapid decrease of the number of double-labelled cells occurred, reaching baseline levels at Day 84 (Fig. 2K). To investigate which of the two axonal arbours of these cells was pruned, it was necessary to analyse the amount of ipsilaterally projecting cells over time.

As the CST is mainly a crossed fibre tract with only ~5% of all CST fibres projecting ipsilaterally in naive adult animals (Brosamle and Schwab, 1997), a persistent increase of ipsilaterally projecting CST fibres could be an important source for functional recovery after a unilateral lesion of the motor cortex. For naive animals $393 \pm 50$ ipsilaterally projecting Fast Blue-labelled cells were observed in the contralesional cortex, corresponding to ~4% of all Fast Blue-labelled cells (Fig. 2I and L). After stroke and treatment with the control antibody no significant increase of ipsilaterally projecting Fast Blue cells was observed at any time point, whereas the anti-Nogo-A treated animals showed an almost 3-fold increase of ipsilaterally projecting cells in the contralesional cortex at Day 84 post lesion ($1094 \pm 110.1$, $P < 0.001$, unpaired two-tailed Student's *t*-test). The amount of ipsilaterally projecting cells, projecting to the denervated side of the spinal cord, reached significance after 21 days post-lesion ($P < 0.05$, unpaired two-tailed Student's *t*-test) and continued to increase until 84 days post-lesion (Fig. 2L).

To study the position of the cervically projecting CST cells, in particular the ipsilaterally and the double-projecting cells of the sensorimotor cortex, we mapped their position along the rostrocaudal axis (Fig. 3). Naive animals showed three distinguishable peaks of contralaterally projecting Fast Blue cells, corresponding to the rostral forelimb area, the caudal forelimb area and the secondary somatosensory cortex (Fig. 3A). The photothrombotic stroke lesion affected the hemisphere massively, and only ~4–9% of all contralaterally projecting Fast Blue cells were spared by the lesion. These cells were mainly located in the most rostral part of the rostral forelimb area and at the lateral rim of the caudal forelimb area and the secondary somatosensory cortex. No significant difference between the two treatment groups was observed at any time point (Fig. 3A). The tracing efficiency for contralaterally projecting Diamidino Yellow cells was slightly lower as for Fast Blue cells (high efficiency tracer Fast Blue for ipsilaterally projecting cells), but the same three distinguishable peaks were observed. In naive animals the rostral forelimb area consisted of ~5% of all Diamidino Yellow cells, whereas the caudal forelimb area consisted of ~79% of all Diamidino Yellow cells and the secondary somatosensory cortex of ~16% of all Diamidino Yellow cells (Fig. 3B). After stroke, both treatment groups showed plastic rearrangements over time, with a massive increase of cells in the caudal and rostral forelimb area (Fig. 3B). This increase of contralateral projecting cells was around 2.5-fold for the rostral forelimb and 2-fold for the caudal forelimb area (84 days post-lesion). Despite the general increase for both groups, the caudal forelimb area was still comprised of ~79% of all contralateral projecting cells (anti-BrdU: 79%, anti-Nogo-A: 78%), whereas the rostral forelimb region increased proportionally (anti-BrdU: 10%, anti-Nogo-A: 14%) at 84 days after lesion.

The distribution of double-labelled cells for naive animals was almost uniform over the entire forelimb area and did not show peaks at specific locations (Fig. 3C). After stroke and treatment with an anti-BrdU antibody a similar distribution as for naive

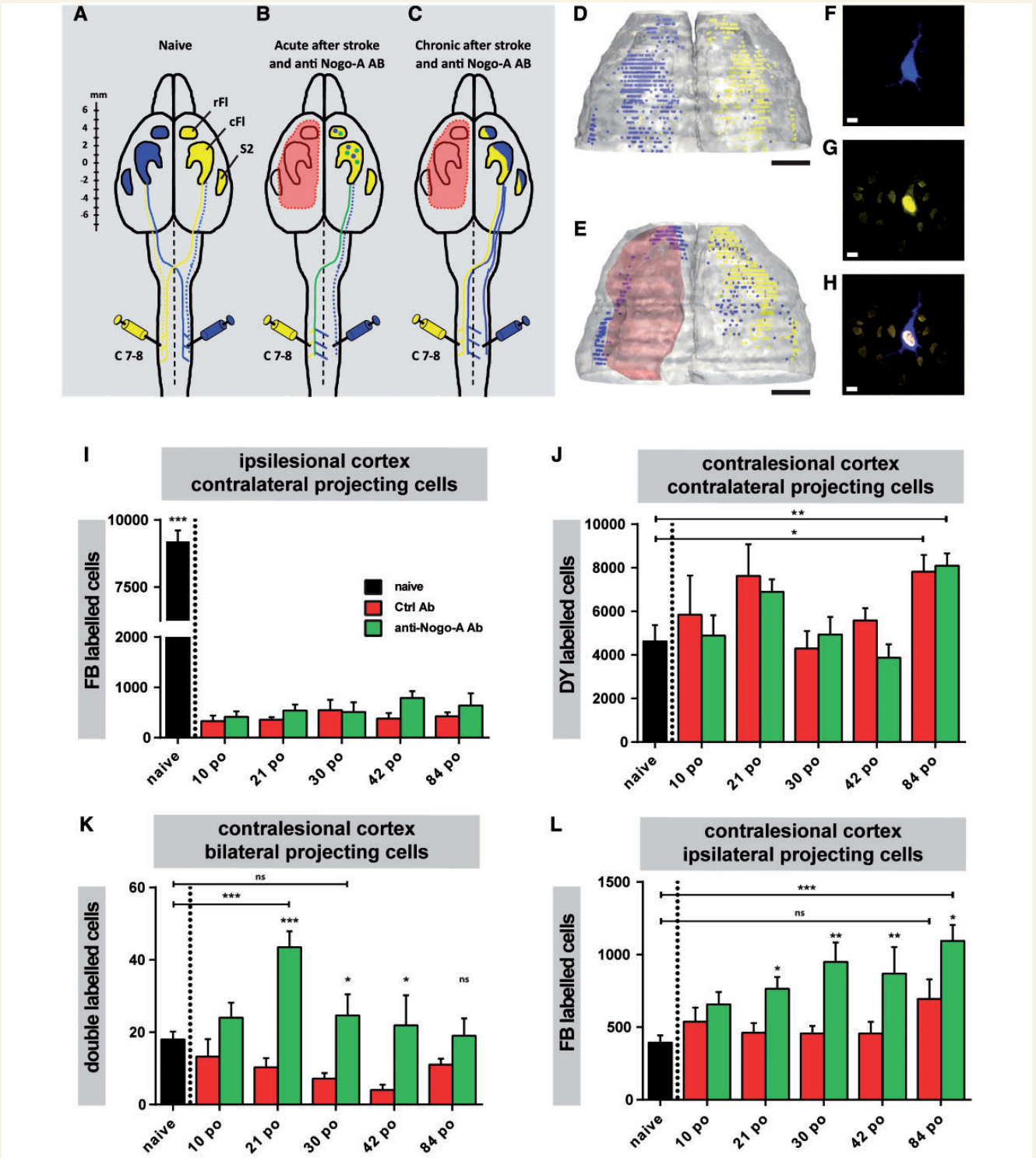


**Figure 2** The somatotopic representation and cell count of the forelimb motor cortex after bilateral retrograde tracing from the cervical level C7–C8 (Fast Blue: right spinal cord, Diamidino Yellow: left spinal cord) of naive animals and animals at different time points after stroke and control antibody or anti-Nogo-A antibody treatment. The CST of naive animals is mainly a crossed pathway (**A**) therefore the left forelimb area (rFL = rostral forelimb, cFL = caudal forelimb, S2 = secondary somatosensory cortex) will be mostly labelled with Fast Blue-labelled cells, whereas the right forelimb area will be mostly labelled with Diamidino Yellow-labelled cells (**A** and **D**). Early after a unilateral stroke lesion (red outline) and treatment with an anti-Nogo-A antibody (**B**) a recrossing of fibres from the spared CST was observed. Double labelled cells (**F** = Fast Blue, **G** = Diamidino Yellow, **H** = merge) and an increase in ipsilateral projecting Fast Blue cells (contralesional cortex) indicate plastic changes. At more chronic time points (**C** and **E**), pruning has reduced the abnormal double projections and only an increase in ipsilateral Fast Blue projecting cells was observed. (**D**) Dorsal view of a 3D reconstruction of a representative naive animal after bilateral cervical tracing with Fast Blue and Diamidino Yellow. (**E**) Dorsal view of a 3D reconstruction of a

(continued)

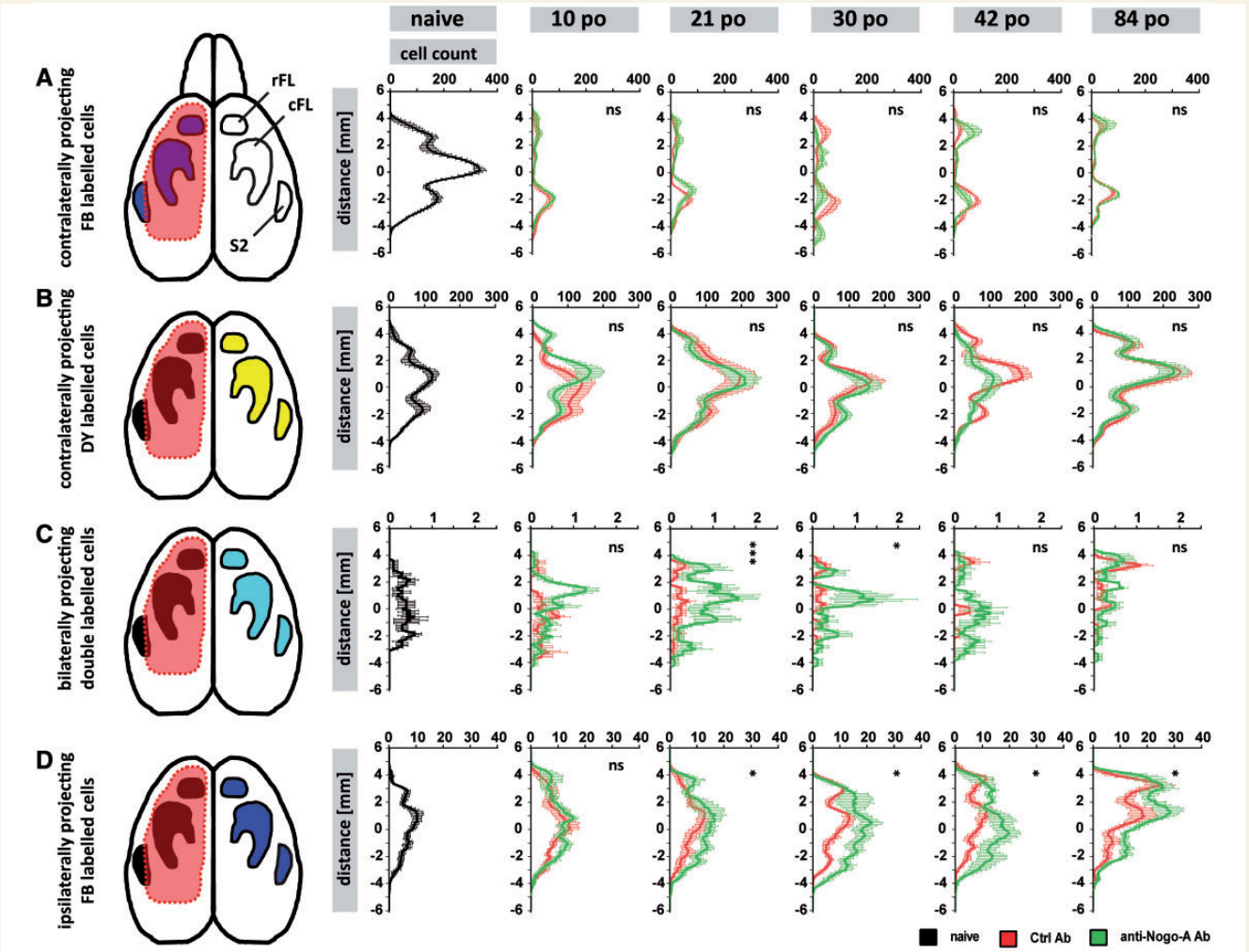


**Figure 3** The anterior-posterior distribution and the amount of contralaterally projecting, spared Fast Blue (FB) cells in the ipsilesional cortex (**A**), contralaterally projecting Diamidino Yellow cells in the contralesional cortex (**B**), bilaterally projecting double-labelled cells in the contralesional cortex (**C**) and ipsilaterally projecting Fast Blue-labelled cells in the contralesional cortex (**D**) in relation to bregma (0 mm anterior-posterior). Black group = naive animals ($n = 6$), red group = stroke lesion and anti-BrdU treatment [10 days postoperative (po) $n = 7$, 21 days postoperative $n = 7$, 30 days postoperative $n = 5$, 42 days postoperative $n = 6$, 84 days postoperative $n = 6$], green group = stroke lesion and anti-Nogo-A treatment (10 days postoperative $n = 7$, 21 days postoperative $n = 6$, 30 days postoperative $n = 5$, 42 days postoperative $n = 5$, 84 days postoperative $n = 6$). Red outline indicates area affected by photothrombotic stroke. rFL = rostral forelimb, cFL = caudal forelimb and S2 = secondary somatosensory cortex. Data are presented as sliding window average of mean ± SEM. Statistical evaluation was carried out with two-way repeated measures ANOVA followed by Bonferroni *post hoc*, asterisks indicate significances: $*P < 0.05$, $***P < 0.001$.

**Figure 2** Continued

representative animal after stroke and treatment with anti-Nogo-A (red outline, 84 days post-lesion) and bilateral cervical tracing with Fast Blue and Diamidino Yellow. This increase of ipsilateral projections is a result of midline crossing fibres and strengthening of the pre-existing ipsilateral projections and induces a somatotopic reorganization of the contralesional cortex. (**I**) Amount of contralateral projecting Fast Blue-labelled cells spared by the stroke lesion in the ipsilesional cortex at different time points after stroke and for the naive situation. (**J**) Amount of contralateral projecting Diamidino Yellow cells in the contralesional cortex at different time points after stroke and for the naive situation. (**K**) Amount of double-labelled cells (projecting to both sides of the spinal cord) in the contralesional cortex at different time points after stroke and for the naive situation. (**L**) Amount of ipsilaterally projecting Fast Blue cells in the contralesional cortex at different time points after stroke and for the naive situation. Black group = naive animals ($n = 6$), red group = stroke lesion and anti-BrdU treatment [10 days postoperative (po) $n = 7$, 21 days postoperative $n = 7$, 30 days postoperative $n = 5$, 42 days postoperative $n = 6$, 84 days postoperative $n = 6$], green group = stroke lesion and anti-Nogo-A treatment (10 days postoperative $n = 7$, 21 days postoperative $n = 6$, 30 days postoperative $n = 5$, 42 days postoperative $n = 5$, 84 days postoperative $n = 6$). Data are presented as means ± SEM. Statistical evaluation was carried out with unpaired two-tailed Student's *t*-test, asterisks indicate significances: $*P < 0.05$, $**P < 0.01$, $***P < 0.001$. Scale bars: **D** and **E** = 2 mm; **F–H** = 10 μm.

animals was observed, except for Day 84 after lesion when an almost 3-fold increase in double-labelled cells was detected in the rostral forelimb area. For anti-Nogo-A treated animals a massive increase in double-labelled cells, with peaks in the rostral and caudal forelimb area, was observed at Day 21 post-lesion. For the rostral forelimb area this increase was >3-fold, compared with the naive situation, whereas for the caudal forelimb area it was >2-fold. This was followed by a decrease of double-labelled cells until Day 42, where a difference between the groups could no longer be detected (Fig. 3C).

For naive animals a small amount of pre-existing ipsilaterally projecting Fast Blue cells was detected in the contralesional cortex with a peak in the caudal forelimb area (Fig. 3D), where ~84% of all ipsilaterally projecting cells were located (rostral forelimb: ~5% and secondary somatosensory cortex: ~11%). After stroke and treatment with the control anti-BrdU antibody a 4-fold increase in ipsilaterally projecting Fast Blue cells was observed for the rostral forelimb area at Day 84. The caudal forelimb and the secondary somatosensory cortex were almost unchanged (Fig. 3D). Animals that were treated with an anti-Nogo-A antibody showed a continuous increase of ipsilaterally projecting cells over time in all forelimb regions. At Day 84 after lesion a 5.5-fold increase of cells in the rostral forelimb area, a 2-fold increase in the caudal forelimb area and a 1.5-fold increase in the secondary somatosensory area were detected. At this time point the rostral forelimb contained ~20% of all ipsilateral cells, whereas the caudal forelimb comprised ~74% of the cells and the secondary somatosensory cortex contained ~6% of all ipsilateral cells.

Average 2D false colour-coded projection heat maps of the position and density of contralaterally and ipsilaterally projecting cells were obtained for all naive animals and for all animals from the chronic time point (84 Days post lesion) (Fig. 4). For contralateral projections the majority of CST fibres originate in the caudal forelimb area with smaller proportions coming from the rostral forelimb area and the secondary somatosensory area (Fig. 4A). In naive rats only a small fraction of fibres project to the ipsilateral side and their origin is almost exclusively in the caudal forelimb region (Fig. 4B). The increase in ipsilateral projections observed

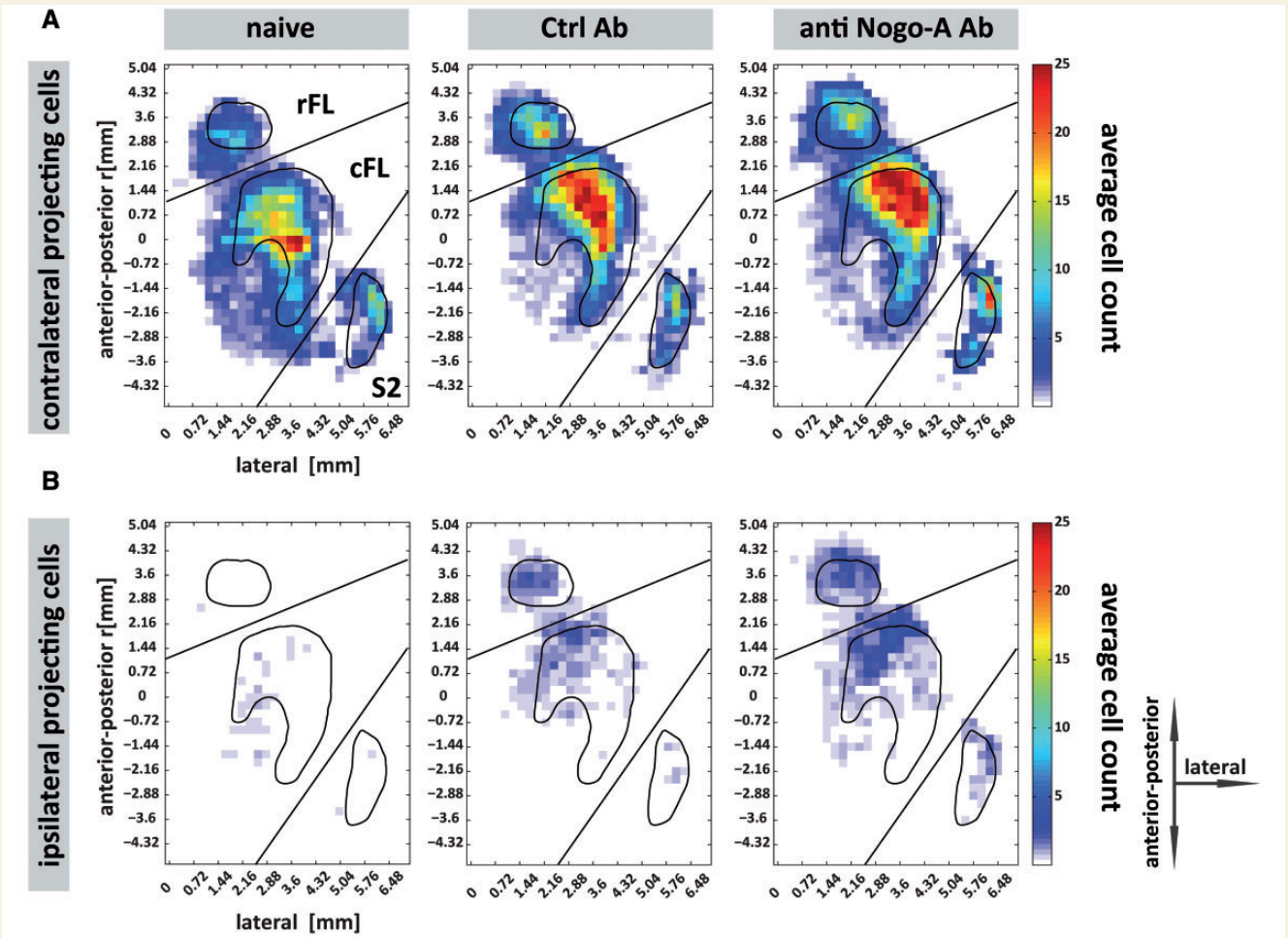


**Figure 4** Average false colour coded heat map of the spatial distribution (dorsal 2D view) and cell density of contralateral projecting Diamidino Yellow cells (**A**) and ipsilateral projecting Fast Blue cells (**B**), for naive animals ($n = 6$) and animals 84 days post-lesion (control antibody $n = 6$ and anti-Nogo-A antibody $n = 6$), in the contralesional cortex in relation to bregma (0 mm anterior-posterior and medio-lateral). Straight lines indicate the boundaries of the rostral forelimb (rFL), the caudal forelimb area (cFL) and the secondary somatosensory cortex = S2.

after a unilateral stroke lesion originates, to a large extent, from the rostral forelimb area (Fig. 4B). In the caudal forelimb region, the ipsilaterally projecting neurons are located more medially than the bulk of the contralaterally projecting cells, suggesting that the more medially located motor CST component might be more plastic than the lateral, mostly sensory part (Fig. 4B). Anti-Nogo-A treated animals showed the highest density of ipsilaterally and contralaterally projecting CST neurons in all analysed cortical regions.

These results demonstrate an enhanced outgrowth/sprouting of the contralesional CST in anti-Nogo-A treated animals with fibres crossing the midline and innervating the denervated half of the spinal cord. These plastic changes are followed by a somatotopic reorganization of the unlesioned hemisphere and the formation of an ipsilateral forelimb area.

## Cortical reorganization is caused by midline crossing fibres and sprouting ventral corticospinal tract fibres in the cervical spinal cord

To study the course of the increased ipsilateral CST fibres, we injected the anterograde tracers biotin-dextran-tetramethylrhodamine (Fluoro Ruby) into the contralesional rostral forelimb area and biotin-dextran-fluorescein (Mini Emerald) into the contralesional caudal forelimb area of chronically recovered animals that were either treated with anti-Nogo-A or control antibody. CST fibres can reach the denervated cervical spinal cord in two ways: as originally contralateral fibres that recross the spinal cord midline segmentally, or as uncrossed, pre-existing ipsilaterally projecting axons. The latter are predominantly found in the medial part of the ventral funiculus (Brosamle and Schwab, 1997), and we counted the number of intersections of collaterals of these fibres at the grey/white matter boundary of the ventral funiculus as a measure of innervation of the cervical grey matter by ventral CST fibres. Our anterograde tracing experiments showed that both, midline crossing fibres and ventral fibre branches increased in number in response to the anti-Nogo-A treatment. Anti-Nogo-A treated animals had significantly more midline crossing fibres projecting from the rostral forelimb area to the cervical spinal cord than control antibody treated animals ($P < 0.01$, two-way repeated measures ANOVA) (Fig. 5A and E). For pre-existing ipsilateral fibres the main difference between the two groups was observed in more rostral cervical areas (C2–C5), with a constant decline in more caudal regions (Fig. 5B). For midline crossing fibres projecting from the caudal forelimb area a similar observation was made (Fig. 5C and G), with the main difference between the anti-Nogo-A and control antibody treated groups at the cervical level C4 ($P < 0.05$, two-way repeated measure ANOVA followed by Bonferroni *post hoc*), which innervates mostly shoulder and upper arm muscles. Pre-existing ipsilateral CST fibres from the rostral forelimb area increased their cervical grey matter projections >2-fold in anti-Nogo-A treated animals (Fig. 5B and F) compared to control antibody-treated animals ($P < 0.001$, two-way repeated measure ANOVA followed by Bonferroni *post hoc*). The sprouting was again more prominent in the rostral cervical region from C2–C4, but was also observed at caudal cervical areas around C7, where fibres innervate distal arm and forepaw muscles (Fig. 5B). The anterograde tracing from the caudal forelimb area revealed an almost identical picture with more pre-existing ipsilateral, ventral fibres crossing the ventral funiculus grey/white matter border in the anti-Nogo-A treated animals compared with control antibody-treated animals (Fig. 5D and H).

To investigate the dorso-ventral projection pattern of CST fibres from the rostral and caudal forelimb area, we analysed the average CST fibre density (as optical density grey values) on spinal cord cross-sections at the spinal cord level C4 for all animals. The contralateral projection from the intact cortex (left side of the spinal cord) terminated in a dense plexus covering the dorsal layers 3–6, the premotor layer 7 and the ventral horn (Fig. 5I–L). Consistent with the retrograde tracing data, anti-Nogo-A treated animals had the highest density of CST fibres projecting from the caudal forelimb cortex to the contralateral spinal cord (Fig. 5K and L) and showed an increased ipsilateral fibre density (right side of the spinal cord) which closely mimicked the pattern of the contralateral innervation. Typically, the dorsal horn projections were less dense from the rostral forelimb area than from the caudal, sensorimotor forelimb field, where anti-Nogo-A treated rats again had higher fibre densities than control antibody treated animals (Fig. 5I and J).

The combined data from the retrograde and anterograde tracing show increased plasticity of the spared CST from the unlesioned hemisphere with an increase of ipsilaterally projections through midline crossing fibres as well as sprouting of pre-existing ipsilateral fibres after stroke and treatment with anti-Nogo-A antibodies.

## Physiological analysis of the ipsilaterally projecting forelimb area by intracortical microstimulation mapping

To test if the ipsilateral projections from the contralesional hemisphere are functionally relevant, we used intracortical microstimulation in combination with EMG recordings of the contra- and ipsilateral forelimb. We analysed the coordinates, the current and the side of the forelimb response for each stimulation point (100–120 stimulation points with ~40 forelimb responses per animal). The EMG response was classified as a pure contralateral response (when the lowest current induced only a contralateral forelimb response) or as pure ipsilateral response (when the lowest current induced only an ipsilateral forelimb response). These were the two main categories and the combined sum of pure contralateral and pure ipsilateral responses made up 100% of all forelimb responses. However, we wanted to gain additional information about changes of supra-threshold ipsilateral responses, which were not strong enough to induce a pure ipsilateral response, but could still contribute to an ipsilateral movement. Therefore, we investigated a third category, the total ipsilateral response (any ipsilateral forelimb response that was detected additionally to the stronger contralateral response, up to a maximum current of 80 μA). For naive animals the majority of all forelimb responses (from caudal and rostral

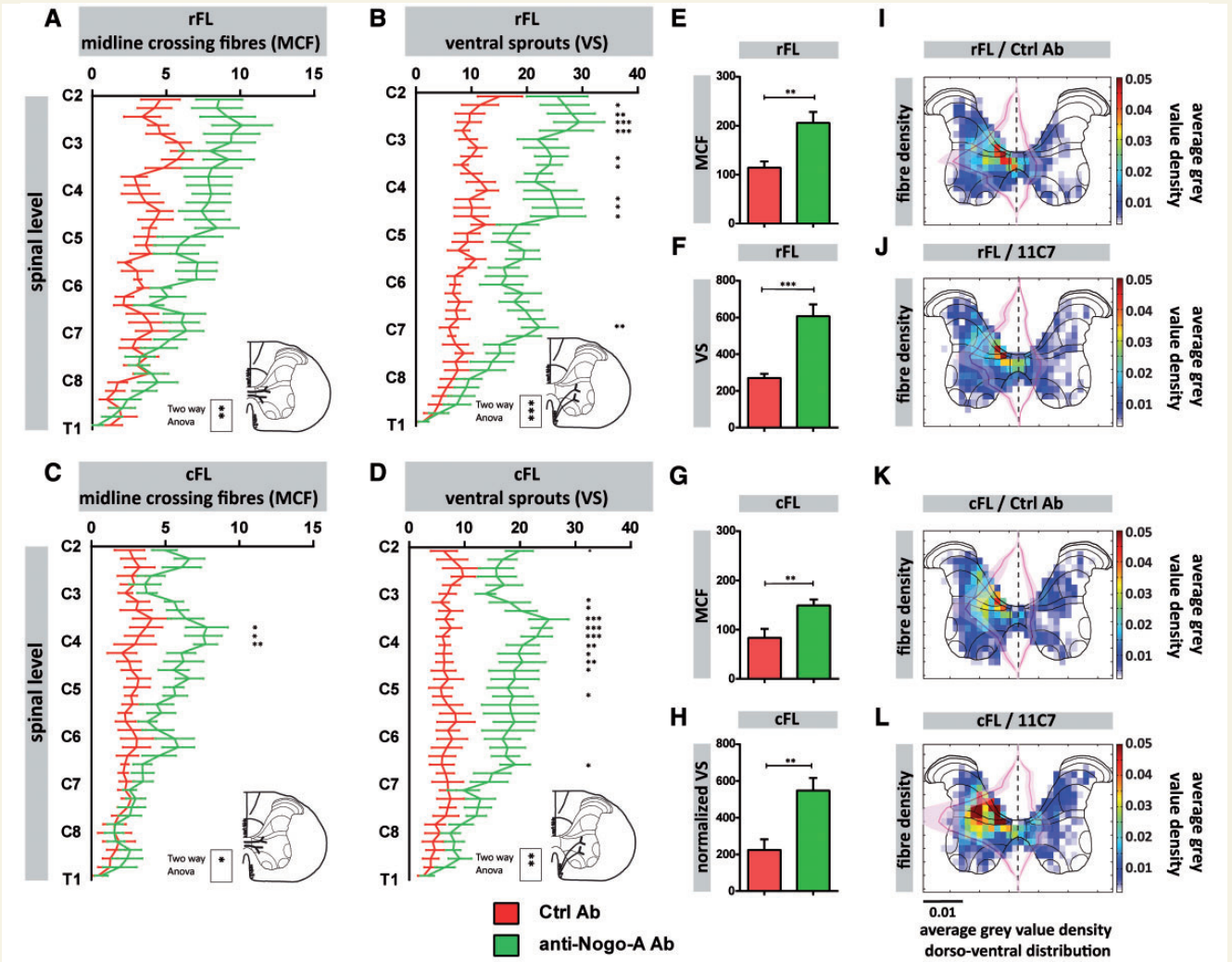


**Figure 5** Amount and distribution of midline crossing fibres (MCF) (**A** and **E**) and sprouting of pre-existing ipsilateral CST fibres (VS) (**B** and **F**) in the grey matter of the cervical enlargement after stroke and anterograde tracing of the rostral forelimb area with tetramethylrhodamine (84 days after the lesion). The amount and distribution of midline crossing fibres (**C** and **G**) and sprouting of pre-existing ipsilateral CST fibres (**D** and **H**) in the grey matter of the cervical enlargement after stroke and anterograde tracing of the caudal forelimb area with fluorescein/biotin (84 days after the lesion). Green group anti-Nogo-A treated animals ($n = 8$) and red group anti-BrdU treated animals ($n = 8$). Average false colour-coded heat maps of grey value fibre density were created for all animals of each treatment group, to indicate the innervation and spatial distribution of CST fibres in the spinal cord laminae at the cervical segment C4 (**I–L**). The red line indicates the fibre distribution along the dorso-ventral axis for both sides of the spinal cord (**I–L**). (**I**) Average false colour-coded heat map of anti-BrdU treated animals traced from the rostral forelimb. (**J**) Average false colour-coded heat map of anti-Nogo-A treated animals traced from the rostral forelimb. (**K**) Average false colour-coded heat map of anti-BrdU treated animals traced from the caudal forelimb. (**L**) Average false colour-coded heat map of anti-Nogo-A treated animals traced from the caudal forelimb area. Statistical evaluation (**A–D**) was carried out with two-way repeated measures ANOVA followed by Bonferroni *post hoc*, asterisks indicate significances: $*P < 0.05$, $**P < 0.01$, $***P < 0.001$. Data are presented as sliding window average of mean ± SEM. Statistical evaluation (**E–H**) was carried out with unpaired two-tailed Student's *t*-test, asterisks indicate significances: $**P < 0.01$, $***P < 0.001$. Data are presented as means ± SEM. Data of the grey value fibre density along the dorso-ventral axis (**I–L**) are presented as mean ± SEM. Data of false colour-coded heat maps of grey value fibre density is presented as mean grey value of each group per voxel.

forelimb area) were pure contralateral (94% ± 4%), and only a few pure ipsilateral responses could be evoked (6% ± 4%, Fig. 6A). However, for ~25% of all forelimb stimulation points a total ipsilateral response could be evoked additionally to the stronger contralateral response (23% ± 9%). Eighty-four days after stroke, animals treated with anti-BrdU showed a similar distribution of forelimb responses, with 98% ± 1% pure contralateral, 2% ± 1% pure ipsilateral and 14% ± 6% total ipsilateral responses. After stroke and treatment with anti-Nogo-A, a decrease of pure contralateral responses (86% ± 4%) due to an ~6-fold increase of pure ipsilateral responses (14% ± 4%) and a 4-fold increase of total ipsilateral responses (57% ± 3%) compared with anti-BrdU treated

animals was detected ($P < 0.001$, unpaired two-tailed Student's *t*-test, Fig. 6A). This increase in ipsilateral muscle responses suggests that the newly formed ipsilateral projections developed large numbers of functional spinal connections as more than half of the cortical stimulation points induced an ipsilateral forelimb muscle response.

The total forelimb response (100%) was further subdivided into responses induced from the rostral (Fig. 6B) and the caudal (Fig. 6C) forelimb areas. For naive animals, as for both treatment groups, the majority of all forelimb responses from the caudal forelimb area were pure contralateral muscle twitches (naive: 81% ± 7%, anti-BrdU: 85% ± 2%, anti-Nogo-A: 77% ± 3%).

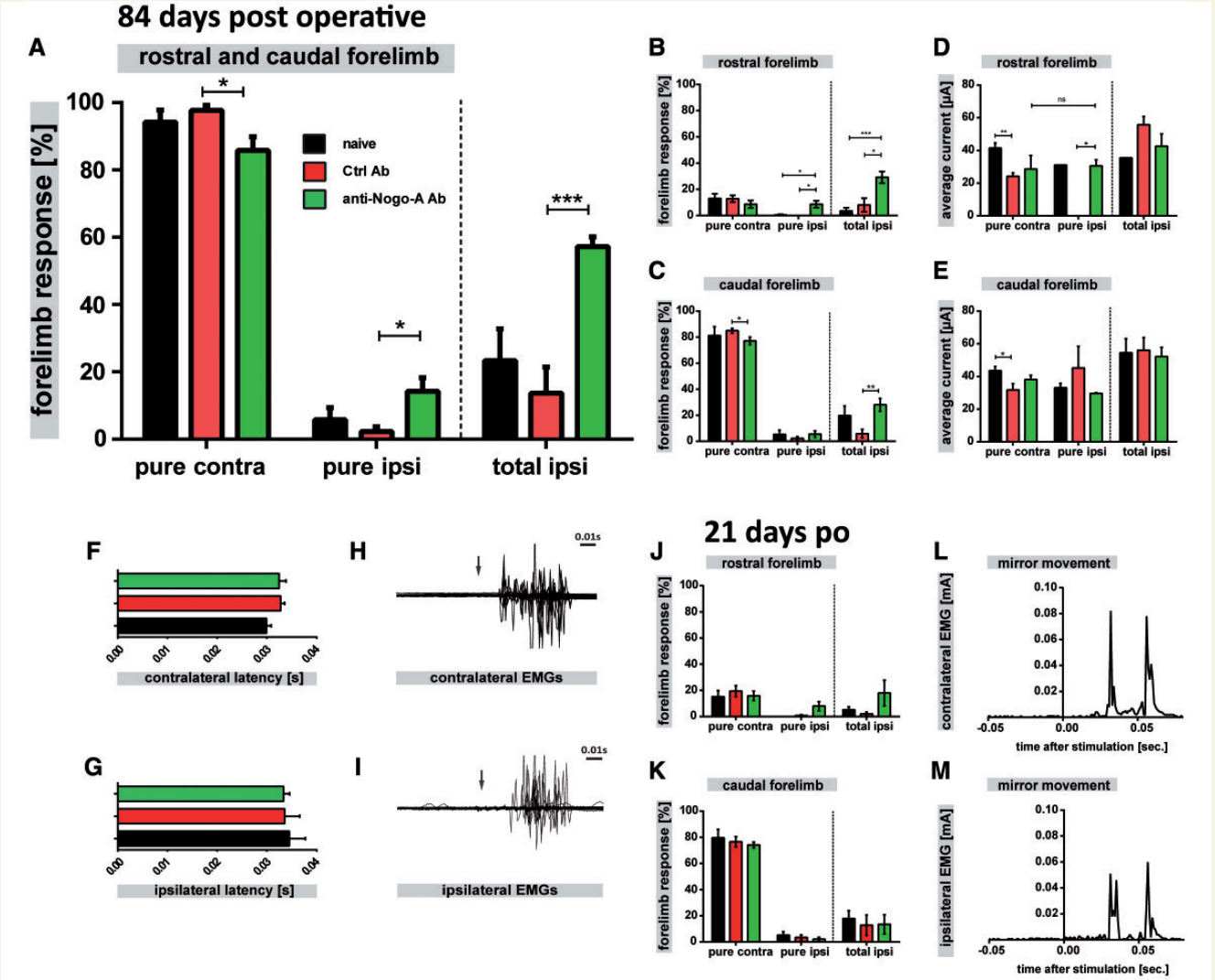


**Figure 6** Percentage of forelimb response (rostral and caudal forelimb) evoked during intracortical microstimulation (ICMS) and recorded by EMG for naive animals (black, $n = 5$), anti-BrdU (red, $n = 6$) and anti-Nogo-A treated animals (green, $n = 5$) 84 days after stroke (**A**). The forelimb EMG response was classified as a pure contralateral response (the lowest current induced a contralateral response), a pure ipsilateral response (the lowest current induced an ipsilateral response) and a total ipsilateral response (any ipsilateral response which was detected independent of the current to a maximum of 80 µA). The total forelimb response was further subdivided into responses from the rostral forelimb area (**B**) and the caudal forelimb area (**C**). The minimum current needed to evoke a movement was analysed for the rostral (**D**) and caudal forelimb area (**E**) and the latency for the induction of a contralateral (**F**) and ipsilateral EMG response (**G**) was detected. (**H** and **I**) Overlay of typical contralateral (**H**) and ipsilateral (**I**) EMG responses of one animal. For ($n = 4$) anti-BrdU and ($n = 4$) anti-Nogo-A treated animals the EMG forelimb response of the rostral forelimb area (**J**) and caudal forelimb area (**K**) 21 days after lesion was evaluated. An example of a full wave rectified bilateral EMG response (mirror movement) of contralateral (**L**) and ipsilateral (**M**) proximal muscle movement is illustrated for an anti-Nogo-A antibody treated animal 21 days after stroke. Data are presented as means ± SEM. Statistical evaluation was carried out with unpaired two-tailed Student's *t*-test, asterisks indicate significances: $*P < 0.05$, $**P < 0.01$, $***P < 0.001$. For the comparison of the pure ipsilateral response (**B**) and the ipsilateral current of the rostral forelimb area (**D**) between anti-Nogo-A and anti-BrdU treated animals, a one sample *t*-test against a theoretical mean was used, as the anti-BrdU animals had no pure ipsilateral response. Asterisks indicate significances: $*P < 0.05$. All data are presented as means ± SEM.

No difference between the groups was detected when the pure ipsilateral response was evaluated (naive: 5% ± 3%, anti-BrdU: 2% ± 1%, anti-Nogo-A: 6% ± 2%). However, for the total ipsilateral responses seen at higher current strengths, the anti-Nogo-A treated group showed a significant increase (28% ± 4.9%) compared with anti-BrdU treated animals (6% ± 3%, $P < 0.01$, unpaired two-tailed Student's *t*-test) (Fig.6C). Interestingly the rostral forelimb area (Fig.6B) of anti-Nogo-A treated animals showed the same amount of pure contralateral responses (9% ± 3%) as pure ipsilateral responses (9% ± 3%). This was significantly different from anti-BrdU treated animals ($P < 0.05$, one sampled Student's *t*-test against hypothetical mean), where no pure ipsilateral response could be detected and naive animals ($P < 0.05$, unpaired two-tailed Student's *t*-test) where only one animal showed a pure ipsilateral response (Fig. 6B). Furthermore, the total ipsilateral response of anti-Nogo-A treated animals increased to 29% ± 4%, compared with 8% ± 5% for anti-BrdU and 3% ± 2% for naive animals.

The current required for inducing a pure contralateral response from the rostral (Fig. 6D) and caudal forelimb area (Fig. 6E) was reduced 84 days after a unilateral stroke lesion compared with naive animals. Pure ipsilateral responses had the same low stimulation threshold as the pure contralateral responses, whereas the thresholds of the total ipsilateral responses in the rostral or caudal forelimb area were generally higher (Fig. 6D and E). The latency of the stimulation to the first peak of a contralateral EMG response was 29.9 ± 1 ms for naive animals, 32.7 ± 0.8 ms for anti-BrdU treated animals and 32.4 ± 0.1 ms for anti-Nogo-A treated animals (Fig. 6F and H). A similar latency with no differences among the treatment groups was observed for ipsilateral EMG responses (34.5 ± 3.2 ms for naive, 33.5 ± 3 ms for anti-BrdU, 33.3 ± 1.2 ms for anti-Nogo-A, Fig. 6G and I).

For chronically recovered animals (84 days after lesion) no forelimb mirror movements were detected. However, when intracortical microstimulation was performed 21 days after the lesion, forelimb mirror movements could be observed for some animals treated with anti-Nogo-A (Fig. 6L and M). These mirror movements were only detected for proximal muscles and only with higher currents. For this early time point after stroke, no significant increase of ipsilateral responses was observed for animals treated with anti-Nogo-A, even if a tendency was visible for the rostral forelimb area (Fig. 6J and K).

## Reappearance of the initial lesion deficit in chronically recovered anti-Nogo-A treated animals after transection of the spared corticospinal tract from the unlesioned hemisphere

To assess the functional role of the spared CST from the unlesioned hemisphere in behaviourally recovered chronic stroke animals, the tract was transected at the pyramidal decussation (Fig. 7A–D) and animals were tested for skilled forelimb reaching. A massive drop in success rate was observed in the anti-Nogo-A treated animals at Day 3 after the lesion, which did not recover (Fig. 7E). Control antibody-treated animals showed no decrease in their (low) success rate after pyramidotomy, even if the more

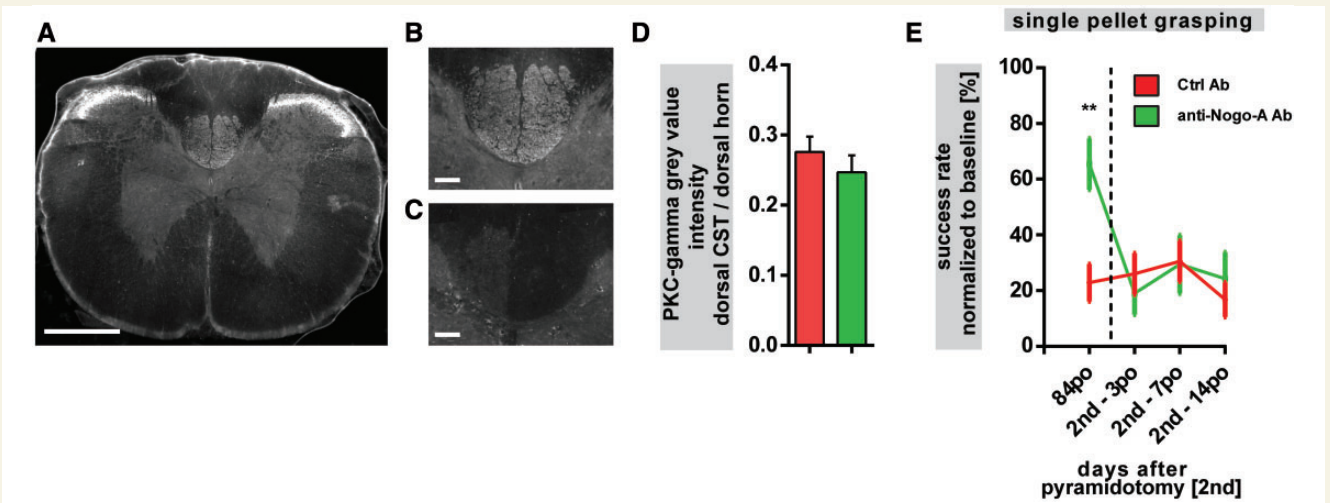


**Figure 7** Success rate in the single pellet grasping task normalized to pre-lesion baseline performance after unilateral photothrombotic stroke lesion and unilateral transection of the spared CST. **(A–C)** Cross sections of the cervical spinal cord stained for the CST marker PKC-$\gamma$ of a naive animal (**A** and **B**) and an animal with stroke followed by a contralesional, unilateral pyramidotomy (98 days post-stroke, 14 days post-pyramidotomy) (**C**). The PKC-$\gamma$ staining labels the dorsal CST and the superficial dorsal horn (**A**), allowing to compare the completeness of the pyramidotomy lesion between the groups using the staining intensities of these two regions (**D**). Success rate in the single pellet grasping task 84 days post-stroke and after stroke followed by pyramidotomy (dashed line) for control antibody-treated animals (red, $n = 10$) and anti-Nogo-A antibody treated animals (green, $n = 9$) (**E**). Data are presented as means ± SEM. Statistical evaluation was carried out with two-way ANOVA repeated measure followed by Bonferroni *post hoc*, asterisks indicate significances: $^{**}P < 0.01$. Scale bars: **A** = 150 μm; **B** and **C** = 50 μm.

detailed 10-point evaluation skilled reaching score showed a significant change in the movement performance (Supplementary Fig. 2). The anti-Nogo-A treated animals dropped to exactly the level of anti-BrdU treated animals and showed a deficit in the 10-point evaluation skilled reaching score comparable to the movement performance observed 3 days after the photothrombotic stroke lesion (Supplementary Fig. 2).

# Discussion

Using a growth enhancing treatment, intrathecal application of anti-Nogo-A antibodies for 2 weeks, after a unilateral subtotal photothrombotic stroke to the sensorimotor cortex, we observed a high degree of functional recovery of fine forelimb movements in adult rats. Such a large amount of recovery after such a severe injury, which destroyed >90% of the forelimb motor cortex, is astonishing and is, without further intervention, usually only observed in neonatally lesioned animals (Whishaw and Kolb, 1988; Kolb *et al.*, 2000). The anti-Nogo-A treated animals continuously improved their success rate at skilled grasping over time, reaching a maximal performance ~6–7 weeks after stroke. Performance then remained stable up to the latest time point tested at 12 weeks. The spontaneous recovery of the control antibody treated group was minimal. To what extent a functional recovery reflects a true recovery of a movement and to what extent compensatory movement patterns contribute to the observed improvement after stroke is a matter of great debate and interest (Krakauer, 2006). Our detailed 10-point grasping analysis indicated a more normal grasping movement for anti-Nogo-A treated animals than for control antibody-treated animals. This observed functional recovery reflects at least partially a true recovery, probably with additional compensatory mechanisms. Movement categories involved with the alignment, advance, aim and grasp of the paw recovered almost fully, whereas other categories such as the supination remained affected. These affected categories were most likely compensated by proximal limb movements in the anti-Nogo-A treated animals, which showed a denser innervation of ipsilaterally projecting fibres into high cervical regions, controlling proximal muscles (Whishaw and Pellis, 1990). Interestingly, the functional recovery of anti-Nogo-A treated animals was paralleled by the enhanced outgrowth of ipsilaterally projecting CST fibres, originating in the contralesional hemisphere. These plastic changes in the contralesional hemisphere were seen as a massive increase of bilaterally projecting double-labelled cells, representing new axonal branches growing over the spinal cord midline. No plastic changes could be observed in the ipsilesional sensory motor cortex, indicating a specific sprouting of the unlesioned CST after very large hemispheric stroke lesions and anti-Nogo-A treatment. Similar results were observed in untreated neonatally lesioned animals (Yoshikawa *et al.*, 2012), an age where the level of growth inhibitory proteins in the CNS, including Nogo-A, are much lower than in the adult CNS (Qiu *et al.*, 2000). Intracortical microstimulation of the contralesional hemisphere 21 days after lesion showed mirror movements in the anti-Nogo-A treated animals. Normally, mirror movements are only found in young children, where they are associated with immature bilateral/ipsilateral projections of CST neurons and a lack of callosal inhibition. In adults mirror movements are unusual and often reflect abnormalities in the projection of CST fibres (Farmer, 2005; Rocca *et al.*, 2005; Srour *et al.*, 2010; Tsuboi *et al.*, 2010).

Our detailed time course study, using retrograde tracing, showed that the initial 2–3-fold increase in double-labelled CST neurons projecting to both sides of the spinal cord in the anti-Nogo-A treated stroke animals was followed by a reduction of this number and an increase in ipsilaterally projecting cells. The increase of ipsilaterally-projecting fibres was partially induced through midline crossing fibres, which were still increased at the chronic time point (84 days post-lesion) for anti-Nogo-A treated animals, as well as a sprouting of pre-existing ipsilateral fibres. This result indicates that the original axonal arbours in the contralateral spinal cord of the sprouting CST fibres were withdrawn to the extent that no tracer uptake was detectable anymore when the fibres innervated the opposite, originally denervated side of the spinal cord. Such a sorting of bilateral projections was observed during developmental maturation of the CST system, where it is regulated by competition dependent mechanisms (Martin, 2005; Friel and Martin, 2007). We speculate that once outgrowth of fibres was induced after stroke and anti-Nogo-A treatment, the spared cortex gained access to the formerly denervated side of the body which led to activity-dependent competition of fibres. Electrical stimulation, constraint induced movement therapy or task-specific training (Brus-Ramer *et al.*, 2007; Maier *et al.*, 2008; Carmel *et al.*, 2010; Starkey *et al.*, 2011; Carmel *et al.*, 2013) had been used to increase plasticity of the spared CST fibres and strengthen functionally important/meaningful connections. As rehabilitation therapy is crucial for recovery after stroke, the combination of a growth and plasticity enhancing anti-Nogo-A antibody treatment, followed by intense rehabilitation, could be a promising future approach for stroke patients to enhance the formation of new neuronal connections and circuits and to shape and stabilize meaningful connections (Starkey and Schwab, 2011). In addition to CST fibres growing across the spinal cord midline, our results also show enhanced branching of the small population of original ipsilateral fibres, in line with earlier observations (Weidner *et al.*, 2001).

The impressive compensatory sprouting of CST fibres from the unlesioned hemisphere that was observed in animals treated with an anti-Nogo-A antibody led to the formation of a greatly expanded ipsilateral forelimb representation in the rostral and caudal forelimb areas (premotor cortex and area 4 in humans; Rouiller *et al.*, 1993) as well as the secondary somatosensory cortex. The newly connected, ipsilaterally projecting cells seemed to be intermixed with the original, contralateral CST neurons. Similar observations were made for animals which received a hemidecortication as neonates and which were bilaterally retrogradely traced as adults (Umeda and Isa, 2011; Yoshikawa *et al.*, 2012). Intracortical microstimulation of the rostral and caudal motor field 84 days after stroke and treatment with an anti-Nogo-A antibody demonstrated their influence on ipsilateral muscle activation, as 57% of all forelimb stimulation points lead to an ipsilateral response (14% in control antibody-treated rats). In particular the rostral forelimb area reacted in a highly plastic manner after lesion and growth enhancing treatment and

showed a predominant ipsilateral innervation. The influence of this hierarchically higher motor structure on functional recovery was investigated in several recent studies, showing that it is important for the planning of a movement, being densely connected to the caudal forelimb area as well as the spinal cord and being at least partially a bilaterally/ipsilaterally projecting system through the cortico-bulbo-spinal tract, making it a particularly interesting region for plastic reorganization after stroke (Chollet *et al.*, 1991; Frost *et al.*, 2003; Davidson and Buford, 2006; Horenstein *et al.*, 2009; Bestmann *et al.*, 2010; Bashir *et al.*, 2012; Glover *et al.*, 2012; Kantak *et al.*, 2012). This indirect projecting pathway of the cortico-bulbo-spinal tract is known to be involved in the positioning of the body, trunk stability, but also distal wrist and digit movements (Riddle and Baker, 2010; Soteropoulos *et al.*, 2012). These observations together with the increased direct ipsilateral projections from the rostral forelimb area to higher cervical regions, innervating mostly proximal muscles crucial for successful pellet grasping (Whishaw and Pellis, 1990), make the rostral forelimb area a promising region for plasticity based functional recovery. However, further more detailed studies are necessary to analyse the precise contribution of the rostral and caudal forelimb area on functional recovery after stroke and treatment and to understand the interplay between these areas, including the sensory system (Harrison *et al.*, 2013).

Interestingly, the latencies for contralateral EMG responses did not differ from those of ipsilateral responses, neither in naive nor in stroke and anti-Nogo-A treated animals suggesting a similar connectivity pattern for both sides. Such short ipsilateral latencies were observed for neonatally lesioned animals and human patients with lesions early in life, whereas adult lesioned subjects tend to show a prolonged latency for ipsilateral muscle responses, indicating the involvement of indirect pathways like the cortico-reticulo-spinal tract (Benecke *et al.*, 1991; Muller *et al.*, 1997; Kastrup *et al.*, 2000; Eyre *et al.*, 2001). To test the influence of the direct CST pathway, which was spared by the stroke lesion, we applied a unilateral pyramidotomy lesion 12 weeks after the stroke. The well recovered anti-Nogo-A treated animals showed a massive drop in their skilled forelimb grasping success rate 3 days after the pyramidotomy whereas the control antibody treated animals were unaffected in their low success rate. No further recovery was observed until Day 14 after pyramidotomy. The detailed 10-point evaluation reaching score revealed a comparable deficit for anti-Nogo-A treated animals after pyramidotomy as 3 days after the initial stroke lesion. These results show that the enhanced functional recovery of anti-Nogo-A treated animals was crucially dependent on fibres running in the contralesional CST. For control antibody-treated animals this fibre tract played only a minor role in functional recovery, even if the general movement pattern, evaluated by 10-point evaluation skilled reaching score, was changed after the pyramidotomy lesion (Bashir *et al.*, 2012). Spontaneous plasticity of the spared CST was insufficient to contribute to behavioural recovery in the single pellet reaching task. These observations indicate that an anti-Nogo-A treatment can increase functional recovery by increasing plasticity of the spared CST and furthermore, that indirect descending pathways, like the cortico-bulbo-spinal pathway, were not involved in the recovery of skilled movement after stroke and anti-Nogo-A treatment. However, further investigations would be necessary to distinguish between the influence of midline crossing fibres and the contribution of sprouting pre-existing ipsilateral projections on functional recovery. Similar observations were made in neonatally operated animals after the transection of the spared CST (Kartje-Tillotson *et al.*, 1987) and in transcranial magnetic stimulation studies in human patients with congenital hemiparesis and good functional recovery (Lotze *et al.*, 2009). These patients showed an increased ipsilateral activation during paretic hand movements and no difference of motor evoked potentials for the affected or unaffected side. A functional blockade, induced through repetitive transcranial magnetic stimulation of the ipsilateral primary motor cortex or dorsal premotor cortex, led to a decrease in temporal precision of finger movements, showing the importance of the contralesional hemisphere. These results indicate a strong influence of direct CST connections on functional recovery after stroke. Nevertheless, phylogenetically older brainstem pathways like the rubro-, vestibulo- and reticulo-spinal pathway are known to influence postural control, proximal limb movements and flexion-biased movements, but their contribution to stroke recovery is less understood (Lemon, 2008). Additional studies are necessary to understand the spontaneous and treatment induced plasticity of these descending pathways and to investigate their influence on functional recovery (Wenk *et al.*, 1999; Papadopoulos *et al.*, 2002).

Recent studies showed that BDNF, Gap-43, ephrin-B3 and other factors are involved with midline crossing fibres, sprouting and functional recovery after a brain injury (Omoto *et al.*, 2011; Ueno *et al.*, 2012), and anti-Nogo-A has been shown to influence the upregulation of different endogen growth factors (Bareyre *et al.*, 2002). Other growth/sprouting enhancing interventions like chondroitinase ABC treatment, intense rehabilitation, electrical stimulation or the manipulation of the intrinsic neuronal growth regulation, e.g. by PTEN or SOCS3 deletion, are also known to induce a massive stimulation of sprouting and regeneration of axons after injury. However, the precise molecular mechanisms that allow fibres to recross over the adult spinal cord midline, e.g. up- and downregulation of particular factors at the spinal cord midline or possible gradients in adjacent areas, are far from being understood. Especially the question, if different growth/sprouting enhancing treatments induce changes of the same molecular factors, or if each treatment has a unique 'fingerprint' is not solved. Further studies including the combination of different treatments would help to deepen our understanding of the mechanisms of recovery.

In conclusion, this study shows substantial functional recovery of forelimb precision movements for adult animals after near complete unilateral stroke to the sensorimotor cortex and anti-Nogo-A antibody treatment which coincides with an anatomical and functional reorganization of the unlesioned hemisphere and its descending CST. Fibres from the unlesioned hemisphere recrossed the spinal cord midline and changed their projection pattern anatomically and functionally from contra- to ipsilateral. Additionally, an increase in pre-existing ipsilateral fibre projections was detected. Newly ipsilaterally projecting neurons are found in the rostral and caudal forelimb areas as well as the secondary somatosensory cortex, with a particularly high contribution of

the rostral, premotor area. These results in rodents guide our understanding of functional recovery based on anatomical plasticity of the CNS after large strokes and show that growth enhancing interventions like the suppression of the growth inhibitory CNS protein Nogo-A can greatly enhance structural rewiring and functional recovery of the injured adult CNS. Human anti-Nogo-A antibodies have entered clinical trials for spinal cord injury and multiple sclerosis, opening the door for new therapeutic approaches also for stroke and brain injury.

## Acknowledgements

The authors thank Christiane Bleul for surgery assistance, Regular Schneider for her help with tissue processing and Hansjörg Kasper and Stefan Giger for technical support.

## Funding

This work was funded by the Swiss National Science Foundation (SNSF) (Grant number 3100AO-122527/1), the National Centre for Competence in Research 'Neural Plasticity and Repair' of the SNSF (Grant number 502213), and the following grants from the 7th Framework Programme FP7/2007-2013 of the European Union: the European Stroke Network (Grant number 201024 and 202213) and the HEALTH – Collaborative Project PLASTICISE (Grant number 223524).

## Supplementary material

Supplementary material is available at *Brain* online.

## References

Bakhai A. The burden of coronary, cerebrovascular and peripheral arterial disease. Pharmacoeconomics 2004; 22 (Suppl 4): 11–18.

Bareyre FM, Haudenschild B, Schwab ME. Long-lasting sprouting and gene expression changes induced by the monoclonal antibody IN-1 in the adult spinal cord. J Neurosci 2002; 22: 7097–110.

Bashir S, Kaeser M, Wyss A, Hamadjida A, Liu Y, Bloch J, et al. Short-term effects of unilateral lesion of the primary motor cortex (M1) on ipsilesional hand dexterity in adult macaque monkeys. Brain Struct Funct 2012; 217: 63–79.

Benecke R, Meyer BU, Freund HJ. Reorganisation of descending motor pathways in patients after hemispherectomy and severe hemispheric lesions demonstrated by magnetic brain stimulation. Exp Brain Res 1991; 83: 419–26.

Bestmann S, Swayne O, Blankenburg F, Ruff CC, Teo J, Weiskopf N, et al. The role of contralesional dorsal premotor cortex after stroke as studied with concurrent TMS-fMRI. J Neurosci 2010; 30: 11926–37.

Biernaskie J, Szymanska A, Windle V, Corbett D. Bi-hemispheric contribution to functional motor recovery of the affected forelimb following focal ischemic brain injury in rats. Eur J Neurosci 2005; 21: 989–99.

Brosamle C, Schwab ME. Cells of origin, course, and termination patterns of the ventral, uncrossed component of the mature rat corticospinal tract. J Comp Neurol 1997; 386: 293–303.

Brus-Ramer M, Carmel JB, Chakrabarty S, Martin JH. Electrical stimulation of spared corticospinal axons augments connections with ipsilateral spinal motor circuits after injury. J Neurosci 2007; 27: 13793–801.

Carmel JB, Berrol LJ, Brus-Ramer M, Martin JH. Chronic electrical stimulation of the intact corticospinal system after unilateral injury restores skilled locomotor control and promotes spinal axon outgrowth. J Neurosci 2010; 30: 10918–26.

Carmel JB, Kimura H, Berrol LJ, Martin JH. Motor cortex electrical stimulation promotes axon outgrowth to brain stem and spinal targets that control the forelimb impaired by unilateral corticospinal injury. Eur J Neurosci 2013; 37: 1090–102.

Chen P, Goldberg DE, Kolb B, Lanser M, Benowitz LI. Inosine induces axonal rewiring and improves behavioral outcome after stroke. Proc Natl Acad Sci USA 2002; 99: 9031–6.

Choi JT, Vining EP, Mori S, Bastian AJ. Sensorimotor function and sensorimotor tracts after hemispherectomy. Neuropsychologia 2009; 48: 1192–9.

Chollet F, DiPiero V, Wise RJ, Brooks DJ, Dolan RJ, Frackowiak RS. The functional anatomy of motor recovery after stroke in humans: a study with positron emission tomography. Ann Neurol 1991; 29: 63–71.

Cramer SC. Repairing the human brain after stroke: I. Mechanisms of spontaneous recovery. Ann Neurol 2008; 63: 272–87.

Davidson AG, Buford JA. Bilateral actions of the reticulospinal tract on arm and shoulder muscles in the monkey: stimulus triggered averaging. Exp Brain Res 2006; 173: 25–39.

Donnan GA, Fisher M, Macleod M, Davis SM. Stroke. Lancet 2008; 371: 1612–23.

Emerick AJ, Neafsey EJ, Schwab ME, Kartje GL. Functional reorganization of the motor cortex in adult rats after cortical lesion and treatment with monoclonal antibody IN-1. J Neurosci 2003; 23: 4826–30.

Eyre JA, Taylor JP, Villagra F, Smith M, Miller S. Evidence of activity-dependent withdrawal of corticospinal projections during human development. Neurology 2001; 57: 1543–54.

Farmer SF. Mirror movements in neurology. J Neurol Neurosurg Psychiatry 2005; 76: 1330.

Farr TD, Whishaw IQ. Quantitative and qualitative impairments in skilled reaching in the mouse (Mus musculus) after a focal motor cortex stroke. Stroke 2002; 33: 1869–75.

Friel KM, Martin JH. Bilateral activity-dependent interactions in the developing corticospinal system. J Neurosci 2007; 27: 11083–90.

Frost SB, Barbay S, Friel KM, Plautz EJ, Nudo RJ. Reorganization of remote cortical regions after ischemic brain injury: a potential substrate for stroke recovery. J Neurophysiol 2003; 89: 3205–14.

Fujimura K, Koga E, Baba S. Neonatal frontal lesion in unilateral hemisphere enhances the development of the intact higher motor cortex in the rat. Brain Res 2003; 965: 51–6.

Glover S, Wall MB, Smith AT. Distinct cortical networks support the planning and online control of reaching-to-grasp in humans. Eur J Neurosci 2012; 35: 909–15.

Grefkes C, Ward NS. Cortical reorganization after stroke: how much and how functional? Neuroscientist 2013; doi: 10.1177/1073858413491147.

Hamadjida A, Wyss AF, Mir A, Schwab ME, Belhaj-Saif A, Rouiller EM. Influence of anti-Nogo-A antibody treatment on the reorganization of callosal connectivity of the premotor cortical areas following unilateral lesion of primary motor cortex (M1) in adult macaque monkeys. Exp Brain Res 2012; 223: 321–40.

Harris NG, Nogueira MS, Verley DR, Sutton RL. Chondroitinase enhances cortical map plasticity and increases functionally active sprouting axons after brain injury. J Neurotrauma 2013; 15: 1257–69.

Harrison TC, Silasi G, Boyd JD, Murphy TH. Displacement of sensory maps and disorganization of motor cortex after targeted stroke in mice. Stroke 2013; 44: 2300–6.

Horenstein C, Lowe MJ, Koenig KA, Phillips MD. Comparison of unilateral and bilateral complex finger tapping-related activation in premotor and primary motor cortex. Hum Brain Mapp 2009; 30: 1397–412.

Johansen-Berg H, Rushworth MF, Bogdanovic MD, Kischka U, Wimalaratna S, Matthews PM. The role of ipsilateral premotor cortex in hand movement after stroke. Proc Natl Acad Sci USA 2002; 99: 14518–23.

Kantak SS, Stinear JW, Buch ER, Cohen LG. Rewiring the brain: potential role of the premotor cortex in motor control, learning, and recovery of

function following brain injury. Neurorehabil Neural Repair 2012; 26: 282–92.
Kartje-Tillotson G, O'Donoghue DL, Dauzvardis MF, Castro AJ. Pyramidotomy abolishes the abnormal movements evoked by intracortical microstimulation in adult rats that sustained neonatal cortical lesions. Brain Res 1987; 415: 172–7.
Kastrup O, Leonhardt G, Kurthen M, Hufnagel A. Cortical motor reorganization following early brain damage and hemispherectomy demonstrated by transcranial magnetic stimulation. Clin Neurophysiol 2000; 111: 1346–52.
Kim JE, Li S, GrandPre T, Qiu D, Strittmatter SM. Axon regeneration in young adult mice lacking Nogo-A/B. Neuron 2003; 38: 187–99.
Kolb B, Cioe J, Whishaw IQ. Is there an optimal age for recovery from motor cortex lesions? II. behavioural and anatomical consequences of unilateral motor cortex lesions in perinatal, infant, and adult rats. Restor Neurol Neurosci 2000; 17: 61–70.
Krakauer JW. Motor learning: its relevance to stroke recovery and neurorehabilitation. Curr Opin Neurol 2006; 19: 84–90.
Kubo T, Yamaguchi A, Iwata N, Yamashita T. The therapeutic effects of Rho-ROCK inhibitors on CNS disorders. Ther Clin Risk Manag 2008; 4: 605–15.
Kumar P, Moon LD. Therapeutics targeting nogo-a hold promise for stroke restoration. CNS Neurol Disord Drug Targets 2013; 12: 200–8.
Lee JK, Kim JE, Sivula M, Strittmatter SM. Nogo receptor antagonism promotes stroke recovery by enhancing axonal plasticity. J Neurosci 2004; 24: 6209–17.
Lemon RN. Descending pathways in motor control. Annu Rev Neurosci 2008; 31: 195–218.
Liebscher T, Schnell L, Schnell D, Scholl J, Schneider R, Gullo M, et al. Nogo-A antibody improves regeneration and locomotion of spinal cord-injured rats. Ann Neurol 2005; 58: 706–19.
Liepert J, Bauder H, Wolfgang HR, Miltner WH, Taub E, Weiller C. Treatment-induced cortical reorganization after stroke in humans. Stroke 2000; 31: 1210–16.
Lotze M, Sauseng P, Staudt M. Functional relevance of ipsilateral motor activation in congenital hemiparesis as tested by fMRI-navigated TMS. Exp Neurol 2009; 217: 440–3.
Maier IC, Baumann K, Thallmair M, Weinmann O, Scholl J, Schwab ME. Constraint-induced movement therapy in the adult rat after unilateral corticospinal tract injury. J Neurosci 2008; 28: 9386–9403.
Martin JH. The corticospinal system: from development to motor control. Neuroscientist 2005; 11: 161–73.
Metz GA, Antonow-Schlorke I, Witte OW. Motor improvements after focal cortical ischemia in adult rats are mediated by compensatory mechanisms. Behav Brain Res 2005; 162: 71–82.
Mori M, Kose A, Tsujino T, Tanaka C. Immunocytochemical localization of protein kinase C subspecies in the rat spinal cord: light and electron microscopic study. J Comp Neurol 1990; 299: 167–77.
Muller K, Kass-Iliyya F, Reitz M. Ontogeny of ipsilateral corticospinal projections: a developmental study with transcranial magnetic stimulation. Ann Neurol 1997; 42: 705–711.
Murase N, Duque J, Mazzocchio R, Cohen LG. Influence of interhemispheric interactions on motor function in chronic stroke. Ann Neurol 2004; 55: 400–9.
Neafsey EJ, Bold EL, Haas G, Hurley-Gius KM, Quirk G, Sievert CF, et al. The organization of the rat motor cortex: a microstimulation mapping study. Brain Res 1986; 396: 77–96.
Nowak DA, Grefkes C, Ameli M, Fink GR. Interhemispheric competition after stroke: brain stimulation to enhance recovery of function of the affected hand. Neurorehabil Neural Repair 2009; 23: 641–56.
Oertle T, van der Haar ME, Bandtlow CE, Robeva A, Burfeind P, Buss A, et al. Nogo-A inhibits neurite outgrowth and cell spreading with three discrete regions. J Neurosci 2003; 23: 5393–406.
Omoto S, Ueno M, Mochio S, Yamashita T. Corticospinal tract fibers cross the ephrin-B3-negative part of the midline of the spinal cord after brain injury. Neurosci Res 2011; 69: 187–95.
Papadopoulos CM, Tsai SY, Alsbiei T, O'Brien TE, Schwab ME, Kartje GL. Functional recovery and neuroanatomical plasticity following middle cerebral artery occlusion and IN-1 antibody treatment in the adult rat. Ann Neurol 2002; 51: 433–41.
Paxinos G, Watson C. The Rat Brain in Stereotactic Coordinates. 5th edn. San Diego: Elsevier Academic Press; 2005.
Puigdellivol-Sanchez A, Prats-Galino A, Ruano-Gil D, Molander C. Fast blue and diamidino yellow as retrograde tracers in peripheral nerves: efficacy of combined nerve injection and capsule application to transected nerves in the adult rat. J Neurosci Methods 2000; 95: 103–10.
Qiu J, Cai D, Filbin MT. Glial inhibition of nerve regeneration in the mature mammalian CNS. Glia 2000; 29: 166–74.
Rehme AK, Fink GR, von Cramon DY, Grefkes C. The role of the contralesional motor cortex for motor recovery in the early days after stroke assessed with longitudinal FMRI. Cereb Cortex 2011; 21: 756–68.
Reinoso BS, Castro AJ. A study of corticospinal remodelling using retrograde fluorescent tracers in rats. Exp Brain Res 1989; 74: 387–94.
Riddle CN, Baker SN. Convergence of pyramidal and medial brain stem descending pathways onto macaque cervical spinal interneurons. J Neurophysiol 2010; 103: 2821–32.
Rocca MA, Mezzapesa DM, Comola M, Leocani L, Falini A, Gatti R, et al. Persistence of congenital mirror movements after hemiplegic stroke. AJNR Am J Neuroradiol 2005; 26: 831–4.
Rouiller EM, Liang FY, Moret V, Wiesendanger M. Trajectory of redirected corticospinal axons after unilateral lesion of the sensorimotor cortex in neonatal rat; a phaseolus vulgaris-leucoagglutinin (PHA-L) tracing study. Exp Neurol 1991; 114: 53–65.
Rouiller EM, Moret V, Liang F. Comparison of the connectional properties of the two forelimb areas of the rat sensorimotor cortex: support for the presence of a premotor or supplementary motor cortical area. Somatosens Mot Res 1993; 10: 269–89.
Schaechter JD, Perdue KL. Enhanced cortical activation in the contralesional hemisphere of chronic stroke patients in response to motor skill challenge. Cereb Cortex 2008; 18: 638–47.
Seymour AB, Andrews EM, Tsai SY, Markus TM, Bollnow MR, Brenneman MM, et al. Delayed treatment with monoclonal antibody IN-1 1 week after stroke results in recovery of function and corticorubral plasticity in adult rats. J Cereb Blood Flow Metab 2005; 25: 1366–75.
Simonen M, Pedersen V, Weinmann O, Schnell L, Buss A, Ledermann B, et al. Systemic deletion of the myelin-associated outgrowth inhibitor Nogo-A improves regenerative and plastic responses after spinal cord injury. Neuron 2003; 38: 201–11.
Soleman S, Yip PK, Duricki DA, Moon LD. Delayed treatment with chondroitinase ABC promotes sensorimotor recovery and plasticity after stroke in aged rats. Brain 2012; 135: 1210–23.
Soteropoulos DS, Williams ER, Baker SN. Cells in the monkey pontomedullary reticular formation modulate their activity with slow finger movements. J Physiol 2012; 590: 4011–27.
Srour M, Riviere JB, Pham JM, Dube MP, Girard S, Morin S, et al. Mutations in DCC cause congenital mirror movements. Science 2010; 328: 592.
Starkey ML, Bleul C, Maier IC, Schwab ME. Rehabilitative training following unilateral pyramidotomy in adult rats improves forelimb function in a non-task-specific way. Exp Neurol 2011; 232: 81–89.
Starkey ML, Schwab ME. Anti-Nogo-A and training: can one plus one equal three? Exp Neurol 2011; 235: 53–61.
Starkey ML, Bleul C, Zorner B, Lindau NT, Mueggler T, Rudin M, et al. Back seat driving: hindlimb corticospinal neurons assume forelimb control following ischaemic stroke. Brain 2012; 135: 3265–81.
Stoeckel MC, Binkofski F. The role of ipsilateral primary motor cortex in movement control and recovery from brain damage. Exp Neurol 2010; 221: 13–17.
Taub E, Uswatt G. Constraint-Induced Movement therapy: answers and questions after two decades of research. NeuroRehabilitation 2006; 21: 93–5.

Thallmair M, Metz GA, Z'Graggen WJ, Raineteau O, Kartje GL, Schwab ME. Neurite growth inhibitors restrict plasticity and functional recovery following corticospinal tract lesions. Nat Neurosci 1998; 1: 124–31.

Tsai SY, Papadopoulos CM, Schwab ME, Kartje GL. Delayed Anti-Nogo-A therapy improves function after chronic stroke in adult rats. Stroke 2010; 42: 186–90.

Tsuboi F, Nishimura Y, Yoshino-Saito K, Isa T. Neuronal mechanism of mirror movements caused by dysfunction of the motor cortex. Eur J Neurosci 2010; 32: 1397–406.

Ueno M, Hayano Y, Nakagawa H, Yamashita T. Intraspinal rewiring of the corticospinal tract requires target-derived brain-derived neurotrophic factor and compensates lost function after brain injury. Brain 2012; 135: 1253–67.

Umeda T, Isa T. Differential contributions of rostral and caudal frontal forelimb areas to compensatory process after neonatal hemidecortication in rats. Eur J Neurosci 2011; 34: 1453–60.

Watson BD, Dietrich WD, Busto R, Wachtel MS, Ginsberg MD. Induction of reproducible brain infarction by photochemically initiated thrombosis. Ann Neurol 1985; 17: 497–504.

Weidner N, Ner A, Salimi N, Tuszynski MH. Spontaneous corticospinal axonal plasticity and functional recovery after adult central nervous system injury. Proc Natl Acad Sci USA 2001; 98: 3513–18.

Weinmann O, Schnell L, Ghosh A, Montani L, Wiessner C, Wannier T, et al. Intrathecally infused antibodies against Nogo-A penetrate the CNS and downregulate the endogenous neurite growth inhibitor Nogo-A. Mol Cell Neurosci 2006; 32: 161–73.

Wenk CA, Thallmair M, Kartje GL, Schwab ME. Increased corticofugal plasticity after unilateral cortical lesions combined with neutralization of the IN-1 antigen in adult rats. J Comp Neurol 1999; 410: 143–57.

Whishaw IQ, Kolb B. Sparing of skilled forelimb reaching and corticospinal projections after neonatal motor cortex removal or hemidecortication in the rat: support for the Kennard doctrine. Brain Res 1988; 451: 97–114.

Whishaw IQ, Pellis SM. The structure of skilled forelimb reaching in the rat: a proximally driven movement with a single distal rotatory component. Behav Brain Res 1990; 41: 49–59.

Wiessner C, Bareyre FM, Allegrini PR, Mir AK, Frentzel S, Zurini M, et al. Anti-Nogo-A antibody infusion 24 hours after experimental stroke improved behavioral outcome and corticospinal plasticity in normotensive and spontaneously hypertensive rats. J Cereb Blood Flow Metab 2003; 23: 154–65.

Yoshikawa A, Atobe Y, Takeda A, Kamiya Y, Takiguchi M, Funakoshi K. A retrograde tracing study of compensatory corticospinal projections in rats with neonatal hemidecortication. Dev Neurosci 2012; 33: 439–47.